https://doi.org/10.5194/cp-2022-96
Preprint. Discussion started: 24 January 2023

Climate of the Past Discussions

A global compilation of diatom silica oxygen isotope records from lake sediment – trends, and implications for climate reconstruction

Philip Meister[1], Anne Alexandre[2], Hannah Bailey[3], Philip Barker[4], Boris K. Biskaborn[1], Ellie Broadman[5], Rosine Cartier[2,6], Bernhard Chapligin[1], Martine Couapel[2], Jonathan R. Dean[7], Bernhard Diekmann[1,8], Poppy Harding[9], Andrew C. G. Henderson[10], Armand Hernandez[11], Ulrike Herzschuh[1,12,13], Svetlana S. Kostrova[1], Jack Lacey[14], Melanie J. Leng[14, 15], Andreas Lücke[16], Anson W. Mackay[17], Eniko Katalin Magyari[18], Biljana Narancic[19,1], Cécile Porchier[20], Gunhild Rosqvist[21], Aldo Shemesh[22], Corinne Sonzogni[2], George E. A. Swann[23], Florence Sylvestre[2] and Hanno Meyer[1]

1 Alfred Wegener Institute Helmholtz Centre for Polar and Marine Research, Polar Terrestrial Environmental Systems, Potsdam, 14473, Germany
2 Aix Marseille University, CNRS, IRD, INRAE, Coll France, CEREGE, Aix-en-Provence, 13545, France
3 Water, Energy and Environmental Engineering Research Unit, University of Oulu, Oulu, P.O.Box 8000, Finland
4 Lancaster Environment Centre, Lancaster University, Lancaster, LA1 4YQ, United Kingdom
5 Laboratory of Tree-Ring Research, University of Arizona, Tucson, Arizona, AZ 85721-0045, United States
6 Lund University, Department of Geology, Lund, 223 62, Sweden
7 Department of Geography, Geology & Environment, University of Hull, HU6 7RX, United Kingdom
8 Institut für Geowissenschaften, Universität Potsdam, Potsdam, 14476, Germany
9 Royal Holloway, University of London, Department of Geography, Egham Hill, Egham Surrey, TW20 0EX, UK
10 School of Geography, Politics and Sociology, Newcastle University, Newcastle upon Tyne, NE1 7RU, UK, UK.
11 GRICA Group, Centro Interdisciplinar de Química e Bioloxía (CICA), Faculty of Sciences, Universidade da Coruña, A Coruña, 15008, Spain.
12 Institute of Environmental Science and Geography, University of Potsdam, 14476, Germany
13 Institute of Biochemistry and Biology, University of Potsdam, 14476, Germany
14 National Environmental Isotope Facility, Isotope Geosciences Facility, British Geological Survey, Keyworth, Nottingham, NG12 5GG, UK.
15 Centre for Environmental Geochemistry, School of Biosciences, University of Nottingham, Sutton Bonington, LE12 5RD, UK.
16 Institute of Bio- and Geosciences, Agrosphere Institute IBG-3, Forschungszentrum Jülich GmbH, Jülich, 52428, Germany
17 Environmental Change Research Centre, Department of Geography, University College London, London, WC1E 6BT UK.
18 Department of Environmental and Landscape Geography, MTA-MTM-ELTE Research Group for Paleontology, Eötvös Loránd University, Budapest, 1117, Hungary.
19 Laboratoire de Paléoécologie Aquatique, Centre d'Études nordiques & Département de géographie, Université Laval, Laval, G1V 0A6, Canada.
20 Department of Geography, University College London, London, WC1E 6BT, UK.
21 Department of Physical Geography, Stockholm University, Stockholm, 106 91, Sweden.
22 Department of Earth and Planetary Sciences, the Weizmann Institute of Science, Rehovot, 76100, Israel.
23 School of Geography, University of Nottingham, University Park, Nottingham, NG7 2RD, UK

Correspondence to: Philip Meister (philip.meister@awi.de)

https://doi.org/10.5194/cp-2022-96
Preprint. Discussion started: 24 January 2023

Climate of the Past Discussions

Abstract. Oxygen isotopes in biogenic silica ($\delta^{18}O_{BSi}$) from lake sediments allow for quantitative reconstruction of past hydroclimate and proxy–model comparison in terrestrial environments. The signals of individual records have been attributed to different factors, such as air temperature (T_{air}), atmospheric circulation patterns, hydrological changes and lake evaporation. While every lake will have its own set of drivers of d18O, here we explore the extent to which regional or even global signals emerge from a series of palaeoenvironmental records. For this purpose, we have identified and compiled 71 down–core records published to date and complemented these datasets with additional lake basin parameters (e.g. lake water residence time and catchment size) to best characterize the signal properties. Records feature widely different temporal coverage and resolution ranging from decadal–scale records covering the last 150 years to records with multi–millennial scale resolution spanning glacial–interglacial cycles. Best coverage in number of records (N=37) and datapoints (N=2112) is available for northern hemispheric (NH) extra–tropic regions throughout the Holocene (corresponding to Marine Isotope Stage 1; MIS 1). To address the different variabilities and temporal offsets, records were brought to a common temporal resolution by binning and subsequently filtered for hydrologically open lakes with lake water residence times <100 yrs. For mid– to high–latitude (>45° N) lakes, we find common $\delta^{18}O_{BSi}$ patterns during both the Holocene and the Common Era and maxima and minima corresponding to known climate episodes such as the Holocene Thermal Maximum (HTM), Neoglacial Cooling, Medieval Climate Anomaly (MCA) and the Little Ice Age (LIA). These patterns are in line with long–term T_{air} changes supported by previously published climate reconstructions from other archives as well as Holocene summer insolation changes. In conclusion, oxygen isotope records from NH extratopic lake sediments feature a common climate signal at centennial (for CE) and millennial (for Holocene) time scales despite stemming from different lakes in different geographic locations and constitute a valuable proxy for past climate reconstructions.

https://doi.org/10.5194/cp-2022-96
Preprint. Discussion started: 24 January 2023

Climate of the Past Discussions

1 Introduction

1.1 Scientific background

Oxygen isotopes are ubiquitous within the global water cycle and are among the best (hydro)climate proxies worldwide as a result of their potential quantitative interpretability. The most abundant isotope ^{16}O and the rarer isotope ^{18}O are subject to fractionation during water phase transformation and transport processes (Fig. 1). As a result, the relative abundance of these isotopes varies across space, time and reservoirs. The IAEA's standard Vienna Standard Mean Ocean Water (VSMOW) serves as a baseline, closely resembling the isotopic composition of modern seawater. Relative abundance of ^{18}O with regard to ^{16}O is expressed relative to the VSMOW standard as $\delta^{18}O$ and given in units of permil.

Measuring $\delta^{18}O$ in water, vapor, snow and ice allows for quantifying hydroclimatic processes in the global water cycle and has been used to this end for many decades (Dansgaard, 1964; Konecky et al., 2020). In addition to its use in present–day hydrology, $\delta^{18}O$ in environmental archives also serves as a powerful proxy for past hydrology and, in turn, climate. As such, $\delta^{18}O$ is a crucial and quantitative tool for both reconstructions of past climate and for comparison of proxy data to climate–model outputs.

Oxygen isotope records are available from different palaeoenvironmental archives e.g. in glaciers and ice sheets (Andersen et al., 2004), permafrost (Meyer et al., 2015b), marine (Spielhagen and Mackensen, 2021) and lacustrine (Leng, 2006) environments as well as different materials, such as carbonates (Kwiecien et al., 2014), silicates (Leng, 2006), biomarkers (Lasher et al., 2017), cellulose (Wolfe et al., 2007), glacier (Andersen et al., 2004) and ground ice (Opel et al., 2017). Therefore, oxygen isotopes offer the possibility for directly comparing data from different palaeoenvironmental archives.

The predictability of isotope fractionation processes in the water cycle due to clear physical constraints allows for using $\delta^{18}O$ not only as a quantitative tool for past (hydro)climate reconstructions, but also for implementing $\delta^{18}O$ in global climate models (e.g. Danek et al. 2021). However, challenges persist in understanding and comparing data and model outputs, partly due to complex signal formation in environmental archives (Danek et al., 2021).

Lake sediments are prominent and widespread archives in terrestrial environments (Leng, 2006; Biskaborn et al., 2016; Subetto et al., 2017). Like glaciers and ice caps, lakes may record the isotopic signature of past precipitation (Shemesh et al., 2001a). The signal formation in lakes, however, is fundamentally different from that in glaciers and ice caps with the lake water body acting as a buffer of the enclosed (hydro)climate signal, influenced by factors such as, catchment hydrology, lake ontogeny, and sediment accumulation rates (Bittner et al., 2021). While biogenic silica is also found in phytoliths, sponge spicules and chrysophytes, this work focuses exclusively on diatoms. Diatoms are microscopic algae synthesizing their frustules from lake water and the silica dissolved therein, thereby preserving the isotope signal of past lake water. The oxygen isotope composition of the biogenic silica of diatom frustules ($\delta^{18}O_{BSi}$) buried in lake sediment therefore provides valuable insight on past lake water and, in turn, precipitation.

Naturally, the interplay of hydrological and sedimentological processes limits the time span and resolution over which environmental information can be obtained from a lake system, and this varies from lake to lake. Most commonly, $\delta^{18}O_{BSi}$ has

https://doi.org/10.5194/cp-2022-96
Preprint. Discussion started: 24 January 2023

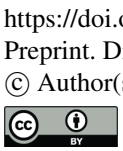

Climate of the Past Discussions
Open Access
EGU

been applied to lake sediments devoid of carbonates. These lakes are especially common in high altitude and high latitude regions (Leng and Barker, 2006).

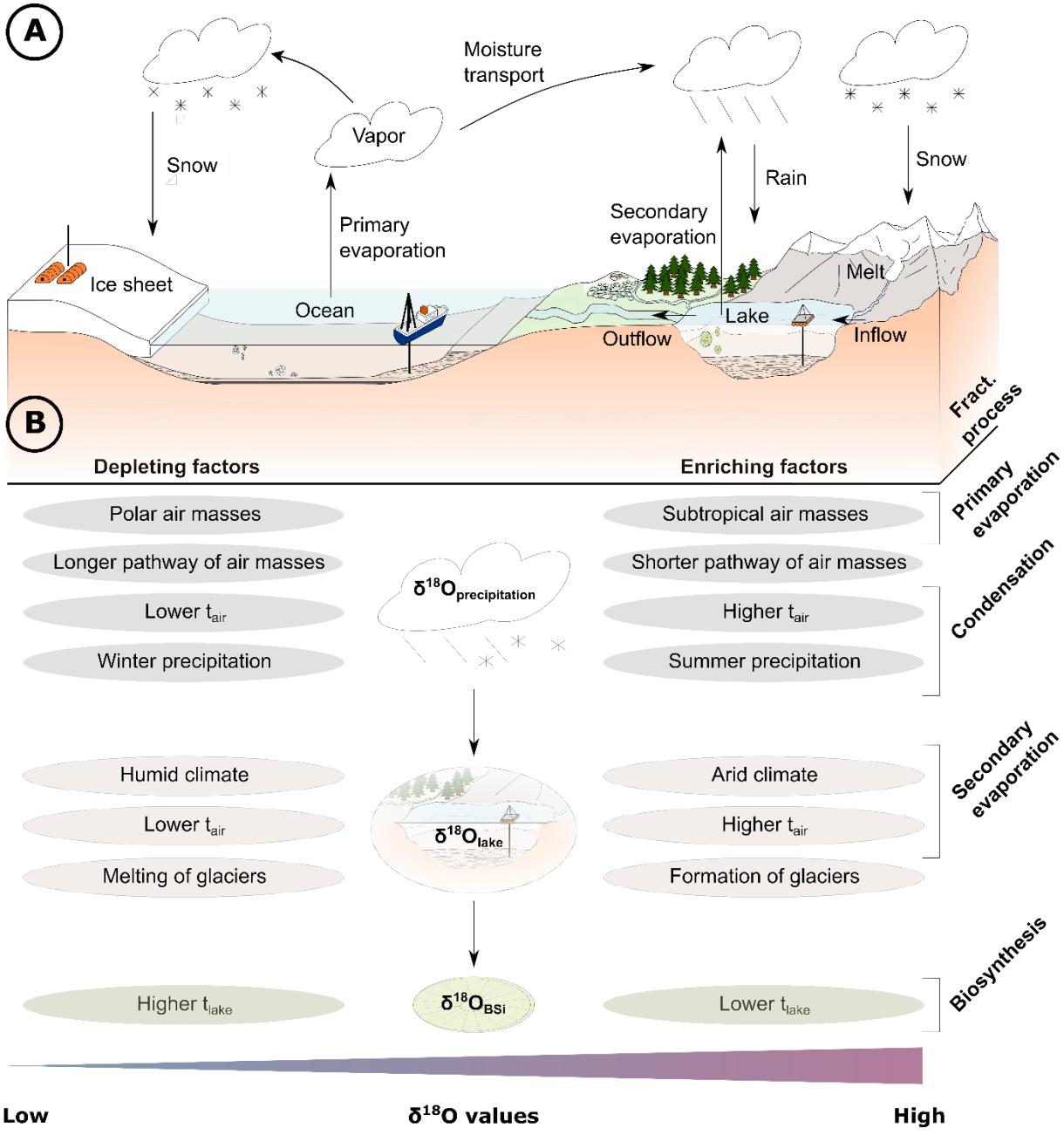

Figure 1. Schematic overview of select reservoirs and processes within the global water cycle influencing the $\delta^{18}O_{BSi}$ signal of records. (a) Overview of the global water cycle with reservoirs and processes. (b) Depleting and enriching factors influencing $\delta^{18}O$ values in precipitation, lake water, and biogenic silica. Corresponding fractionation processes are indicated on the right-hand side.

https://doi.org/10.5194/cp-2022-96
Preprint. Discussion started: 24 January 2023


Climate of the Past Discussions

1.2 Controls on $\delta^{18}O_{BSi}$

As a result of the complex signal formation in $\delta^{18}O_{BSi}$ records, most authors refer to a combination of factors for interpreting a given individual record. A schematic overview of some of the main processes is provided in Fig. 1. Lake water temperature (T_{lake}) imparts a direct effect on $\delta^{18}O_{BSi}$ due to temperature–dependent fractionation during biosynthesis of biogenic silica. The temperature–dependent fractionation coefficients were initially determined for marine environments (Leclerc and Labeyrie, 1987; Matheney and Knauth, 1989) and later adapted for lacustrine sediments, as well. The effect of T_{lake} amounts to ca. – 0.2‰/°C during biosynthesis (Dodd and Sharp, 2010; Moschen et al., 2005). However, the applicability of these calibrations to sedimentary records is debated due to possible disequilibrium between diatom frustules and lake water, as well as taphonomic and diagenetic processes (Leng and Barker, 2006; Ryves et al., 2020; Smith et al., 2016; Tyler et al., 2017).

More commonly, changes in $\delta^{18}O_{BSi}$ are attributed to $\delta^{18}O$ of lake water ($\delta^{18}O_{lake}$) and, with the lake as a buffer, to the isotopic composition of precipitation ($\delta^{18}O_{precipitation}$). Locally, $\delta^{18}O_{precipitation}$ is primarily influenced by air temperature (T_{air}) with a fractionation of 0.7‰/°C on global average (Dansgaard, 1964). On a broader scale, parameters such the moisture source region and atmospheric circulation patterns are important. Air masses transported to a lake are linked to their trajectories and source regions. Hence, changes in $\delta^{18}O_{BSi}$ records may be indicative of changes in atmospheric circulation patterns, also influencing the local ratio of precipitation to evaporation (P/E). The parameter P/E refers to the balance between the amount of precipitation and evaporation within a lake and its catchment. Typically, water loss through evaporation leads to higher $\delta^{18}O_{lake}$ values due to evaporative enrichment, and therefore higher $\delta^{18}O_{BSi}$. Yet, precipitation amount and seasonality (e.g., rain vs. snow) will also strongly impact the isotope signal of the lake water. Disentangling the effects of precipitation and evaporation in $\delta^{18}O_{BSi}$ records is thus a major challenge and therefore some authors commonly refer to P/E–changes in conjunction with other factors (Hernandez et al., 2013; Rosqvist et al., 2013; Broadman et al., 2020a).

Shemesh et al. (2001a) have attributed the $\delta^{18}O_{BSi}$ signal changes of Lake 850 in Swedish Lapland to different contributions of main source regions of precipitation, namely the Atlantic and Arctic Oceans. Indeed, for this location, changes in atmospheric circulation patterns imply changes in both, T_{air} and humidity.

Additionally, $\delta^{18}O_{precipitation}$ may also be linked to shifts in the seasonality of precipitation (Swann et al., 2010; Kostrova et al., 2016; Harding et al., 2020), which is linked to T_{air} change, but also atmospheric circulation patterns (Shemesh et al., 2001a; Jones et al., 2004; Leng et al., 2005; Rosqvist et al., 2013) and, on longer timescales, insolation (Swann et al., 2010; Kostrova et al., 2019; Kostrova et al., 2021). T_{air} as often inferred from $\delta^{18}O_{BSi}$ can, therefore, be a parameter with local, regional and global significance.

Insolation is not strictly speaking an environmental parameter which can be inferred from $\delta^{18}O_{BSi}$ records. It is, however, commonly used as an explanatory variable and underlying driver of Holocene climate change. Insolation can be calculated for any given place throughout time (Laskar et al. 2004), which allows for direct comparison with $\delta^{18}O_{BSi}$ time series. Insolation primarily influences T_{air} and, indirectly, the P/E balance and atmospheric circulation patterns.

https://doi.org/10.5194/cp-2022-96
Preprint. Discussion started: 24 January 2023


Climate of the Past Discussions

Moreover, hydrological processes within a lake's catchment may substantially impact $\delta^{18}O_{lake}$ and hence, $\delta^{18}O_{BSi}$. Some of these processes are closely linked to climate and precipitation patterns described above. Most notable are variations in the amount of snow melt (Mackay et al., 2013; Rosqvist et al., 2013; Meyer et al., 2022) and glacial influx (Meyer et al., 2015a) reaching the lake. Glaciers or snow fields in the hinterland, may provide more melt (with lower/depleted $\delta^{18}O$) in warm phases – countering the influence of warming on $\delta^{18}O_{precipitation}$ (Meyer et al., 2015a).

Other hydrological processes, however, are only indirectly linked to climate. These include the formation and closure of outflows to the lake which change the lake's hydrological setting (Hernandez et al., 2008; Vyse et al., 2020; Bittner et al., 2021). Associated changes in mass–balance of a lake and, thus, P/E–balance may lead to a different $\delta^{18}O_{BSi}$ signal.

In order to interpret a given $\delta^{18}O_{BSi}$, information about the present hydrology is important as it provides insight on which processes influence $\delta^{18}O_{Lake}$ and, in turn, $\delta^{18}O_{BSi}$. Naturally, as the hydrology of a given lake can only offer snapshots of present–day constraints, caution has to be applied when extrapolating these into the past. The isotopic composition of three components is of interest for assessing the signal properties of $\delta^{18}O_{BSi}$ records: (1) $\delta^{18}O$ lake water, (2) $\delta^{18}O$ of inflows to the lake and (3) $\delta^{18}O$ of precipitation. Lake water composition can provide insight on whether lake water is isotopically homogenous, both spatially and at different depths of the lake basin.

Offsets of $\delta^{18}O_{Lake}$ from the Local Meteoric Water Line (LMWL) give hints on whether or not lake evaporation may have had a significant effect on lake water isotopic composition. $\delta^{18}O_{Lake}$ can also be used in conjunction with T_{lake} and the most recent $\delta^{18}O_{BSi}$ value for testing the temperature–dependent fractionation and, in turn, the applicability of the proxy for paleoclimate reconstructions. Complementing the lake water isotopic composition with the isotopic composition of inflow (rivers) provides further information on specific hydrological constraints. For larger lakes and catchments, the different inflows and their effect on the lake's isotopic mass balance have been used for inferring changing hydrology or precipitation regimes in different parts of the catchment (e.g. Mackay et al. 2011).

While the isotopic composition of precipitation provides useful information, it is often not available for field studies and few monitoring studies of precipitation and lake water isotope compositions in combination with $\delta^{18}O_{BSi}$ do exist (Kostrova et al., 2019; Hernandez et al., 2010). A possible workaround can be derived from the GNIP database (IAEA/WMO, 2022) and spatial interpolations thereof, e.g. The Online Isotopes in Precipitation Calculator (Bowen, 2017).

1.3 Sample preparation and measurement

Extracting pure diatom valves (frustules) from lake sediments is a complex process and depends on a sufficiently high diatom concentration in the sediment. Various cleaning procedures for diatom extraction exist, which are mainly based on the use of H_2O_2 for removing organic matter from the sediment and HCl for the removal of carbonate (Chapligin et al., 2012a). Detrital components are often separated by being centrifuged in heavy liquid solution, i.e. Sodium Polytungstate (Morley et al., 2004; Chapligin et al., 2012a). Different procedures in sample preparation, i.e. different temperatures, may result in offsets of measured $\delta^{18}O_{BSi}$ (Swann et al., 2010; Chapligin et al., 2012b; Tyler et al., 2017). Impurities due to incomplete removal of

https://doi.org/10.5194/cp-2022-96
Preprint. Discussion started: 24 January 2023


Climate of the Past Discussions

detrital components may also affect the measured $\delta^{18}O_{BSi}$ (Lamb et al., 2005; Chapligin et al., 2012b). To account for this, the purity of samples is usually assessed prior to measurement by visual inspection or direct measurement of the amount of contaminants of a given sample (Bailey et al., 2018; Broadman et al., 2020a). Fewer studies determine the isotopic composition of detrital contaminants to apply a correction to the measured $\delta^{18}O_{BSi}$ values (Brewer et al., 2008; Mackay et al., 2011; Wilson et al., 2014a; Bittner et al., 2021; Kostrova et al., 2021). Consequently, caution has to be applied when comparing absolute values of different individual $\delta^{18}O_{BSi}$ records, as offsets between individual records may result from both different preparation and measurement techniques and different isotopic signals of the corresponding lake water. The potential and challenges associated with data stemming from different preparation and measurement techniques have already been addressed (Chapligin et al., 2011; Mackay et al., 2011).

1.4 Aim of this work

A comprehensive compilation and assessment of the lake sediment $\delta^{18}O_{BSi}$ records published to date is missing. Due to the crucial role of lake and catchment hydrology in signal formation, such a compilation needs to include individual lake basin parameters, such as lake volume and lake water residence time (t_{res}), in order to provide reliable constraints for interpreting and comparing the individual records. Proxy data compilations have already addressed a lack of standardized metadata, data availability and data uniformity of paleo–data (Pfalz et al., 2021). Such compilations, however, generally do not include $\delta^{18}O_{BSi}$–records and do not provide all relevant lake basin parameters (Kaufman et al., 2020) or have a more limited temporal focus (Konecky et al., 2020). Consequently, no study has yet empirically linked the signal properties of $\delta^{18}O_{BSi}$ records and lake basin parameters in a harmonized dataset.

In order to overcome these gaps, this paper aims at providing a comprehensive compilation and combined statistical evaluation of the lake sediment $\delta^{18}O_{BSi}$–records published to date. We accomplish these objectives by means of the following working steps: 1) collecting available lake sediment $\delta^{18}O_{BSi}$–records published to date, 2) complementing these records with the individual lake basin parameters and 3) assessing the signal properties of $\delta^{18}O_{BSi}$ records with regard to lake basin parameters, in order to 4) identify common spatio–temporal patterns and trends in the $\delta^{18}O_{BSi}$ signals. This effort shall lead to a better understanding of the general constraints for interpreting lake sediment $\delta^{18}O_{BSi}$–records and make these records more readily usable also for proxy–model comparisons. It is, hence, a contribution to bridge the gap between modelling and isotope geochemistry approaches in paleoclimate science.

https://doi.org/10.5194/cp-2022-96
Preprint. Discussion started: 24 January 2023


Climate of the Past Discussions

2. Methods

This study follows a three–stage approach: the first stage (data acquisition) comprises identifying lacustrine $\delta^{18}O_{BSi}$ datasets and publications published to date. A second stage includes acquiring the actual $\delta^{18}O_{BSi}$ datasets and archiving them in a standardized format. Where appropriate, the identified published datasets were arranged into longer continuous records. This includes records from the same sediment core published in different manuscripts and records from different sediment cores from the same lake but similar locations. The third and final stage (record analysis) interprets the actual lacustrine $\delta^{18}O_{BSi}$ isotope records with respect to their hydrological and geographical constraints in order to identify possible common trends and signal properties of all isotope records or smaller spatially or temporally constrained datasets.

Identification and acquisition of the datasets and publications in this work followed an additive approach, i.e. thorough literature survey. We have chosen this approach due to the limited number of laboratories and working groups worldwide measuring $\delta^{18}O_{BSi}$. In this study, we focused exclusively on down–core records from lacustrine sediments. Identified publications and datasets were entered into a uniform metadata table giving one entry to each publication and each dataset. If more than one publication was written about the same sediment core, each of these publications was given a separate entry. Likewise, if one publication presents data from more than one sediment core, each of the sediment cores was given a separate entry to the database.

For each of these entries, metadata on coring procedure, hydrological setting and chronology were supplemented. Data were extracted from the corresponding publication(s), from public repositories or directly from the authors. Hydrological parameters such as catchment area, average depth and t_{res} were additionally obtained from the HydroLAKES database (Messager et al., 2016) and stored as separate variables. For a detailed description on how the values in the HydroLAKES database were created, we refer to Messager et al. (2016). This procedure was necessary because original publications do not always specify all of these parameters and because parameters supplied in original publications may not be consistent. For further analysis and for linking the individual isotope records with lake basin parameters, the HydroLAKES database entries were given preference. Original publications were only used for lakes where no data were available from the HydroLAKES database. The parameter "maximum water depth" was always taken from the original publications since this parameter is not provided by the HydroLAKES database. While the geo–statistical approach of the HydroLAKES database may not provide the most precise values for individual lake basin characteristics, it ensures comparability among the different lake basins analyzed in this study. It also prevents potential issues arising from different authors providing conflicting values for the same lake basin (i.e. Lake Baikal, Lake El'gygytgyn).

Isotope datasets for each of the entries were archived in separate tables specifying depth, age and measured isotope values. Datasets were taken directly from the respective publication, whenever possible. If datasets were not available, within the original publications or as supplements thereof, public repositories (such as www.pangaea.de; ncei.noaa.gov) were searched. In case datasets were unavailable from repositories, the lead authors were contacted directly. In case of published data unavailable from repositories or authors, plots of the original publications were digitized, if possible (Rietti-Shati et al., 1998;

https://doi.org/10.5194/cp-2022-96
Preprint. Discussion started: 24 January 2023


Climate of the Past Discussions

Hu and Shemesh, 2003). Where digitizing plots was not feasible, records were excluded from further consideration; this was the case for Chondrogianni et al. (2004) and Hu et al. (2003).

Chronologies were adapted from the original publications, where available and stored in cal yrs BP format (relative to 1950 CE). Sample ages given in different formats (e.g. b2K or CE) were converted to cal yrs BP. This procedure also applies to radiocarbon–based chronologies. Chronologies were not recalculated because the effect of different ^{14}C–calibrations and different age model approaches is supposedly minor with regard to the aim of this study. This is especially true when considering the fact that high–resolution datasets (annual to decadal resolution) are the exception among all datasets identified. The error introduced by the different age models is, thus, considered minor when compared to the resolution of the datasets. For applications requiring more precise chronologies and better comparability of datasets, we provide the radiocarbon measurements of respective datasets as well. This enables future users to create tailor–made chronologies if needed. Datasets without chronologies were stored using depth notation only.

For further analysis, datasets were partly regrouped and combined to generate longer continuous $\delta^{18}O_{BSi}$ datasets, henceforth referred to as «records». This comprised treating datasets with data from several coring sites or outcrops from the same lake as one single record, in agreement with the author's original interpretation (Quesada et al., 2015; Swann et al., 2018). Data stemming from the same sediment core but published in different manuscripts were combined into single continuous records. This applies to records from Lake Kotokel (Kostrova et al., 2013a; Kostrova et al., 2013b; Kostrova et al., 2014; Kostrova et al., 2016) and Lago Chungará (Hernandez et al., 2008; Hernandez et al., 2010; Hernandez et al., 2011; Hernandez et al., 2013). Likewise, data from different cores presented in different publications but stemming from identical or reasonably similar coring sites were combined to single records. This applies to data from Lake Nar (Dean et al., 2018) and Vuolep Allakasjaure (Rosqvist et al., 2004; Jonsson et al., 2010). Lakes consisting of several basins were generally treated as one; this includes Lake Baikal and several smaller lakes.

For trend analysis and comparison of records with regard to Holocene and Common Era climate, we focused on records from northern hemisphere (NH) extratropic lakes (45–90° N) because these time periods and geographical focus are the only options with a significant number of records which makes an interpretation departing from case studies feasible.

In a first step, records were binned to 1 kyr intervals (for the Holocene) and 200 year intervals (for the CE), respectively. These intervals were chosen based on the temporal resolutions of the original records in order to ensure continuous binned records with no empty bins. Choosing higher resolutions would have resulted in many records having empty bins with no datapoints, thus leading to different temporal resolutions even after binning. The binning was done by calculating the mean value of all samples within the respective age interval for each individual record. For the analysis of the Holocene period, datapoints with ages <150 yrs BP were excluded to eliminate any possible effects of recent warming. Analysis of Common Era climate on the other hand makes use of these datapoints. For an assessment of the timing of Holocene maxima and minima, records covering less than 10 bins were discarded. For trend analysis of Holocene and Common Era climate, records covering less than seven bins were discarded.

https://doi.org/10.5194/cp-2022-96
Preprint. Discussion started: 24 January 2023


Climate of the Past Discussions

In order to eliminate offsets between individual binned records, a mean removal was performed by subtracting the mean of a given binned record from the respective record. After mean removal, two subsequent filtering steps were performed in order to exclude records most prone to secondary lake evaporation. First, a subset consisting only of records from open lakes was created, discarding records from semi–closed lakes, closed lakes and paleo–lakes. In a second step, this open–lakes–subset was filtered by discarding all records with t_{res}>100 years. This threshold was chosen in accordance with previous works classifying lakes and their isotopic signals with respect to hydrologic setting and t_{res} (Leng and Marshall, 2004).

After applying these filters, combined trends for geographical regions (NH, Eurasia, North America) were created by calculating the mean of all records for each bin.

3. Results

3.1 Published datasets

Following a thorough literature survey, a total number of 71 published down–core datasets of $\delta^{18}O_{BSi}$ from 64 sites has been identified. Ever since the first records of $\delta^{18}O_{BSi}$ from lake sediments have been published (Rietti-Shati et al., 1998; Shemesh and Peteet, 1998), there has been a growing research interest, manifest in an increasing number of publications (Fig. A1). Only recently has there been a stagnation of the number of records published. A detailed overview of the identified publications and the records presented therein is provided in Tab. A2.

Most publications give the $\delta^{18}O_{BSi}$ data as time series, as is usual in paleoenvironmental studies. The chronologies rely on a wide variety of dating methods (Fig. A2), with ^{14}C (used on 46 records) being by far the most frequent. For subrecent time periods and shorter time scales, ^{210}Pb and ^{137}Cs are also used extensively (on 21 and 12 records, respectively). Globally or regionally correlated time markers such as tephra layers (Heyng et al., 2015) or high–resolution methods such as varve counts (Rozanski et al., 2010) are used relatively sparsely as they are not available for all time periods and/or lake basins.

3.2 Combined records

We combined separate records stemming from the same lake sites to longer, continuous composite records and yielded a total of 54 combined $\delta^{18}O_{BSi}$ records, seven of which stem from paleolakes (three with and four without chronology) while 49 records stem from present, still existing lakes (44 with and five without chronology). An overview of these combined records is provided in Tab. A1, complemented by metadata of the records and the corresponding lake basins. Each individual record received a number (#X) which is used consistently throughout the text.

The temporal coverage of these combined records (Fig. 2) varies from centennial–scale at Laguna Zacapu (Leng et al., 2005) and a specific study at Lake Baikal (Swann et al., 2018) (records #50, #51) to glacial–interglacial cycles e.g. 250 kyrs at Lake El'gygytgyn (#3, (Chapligin et al., 2012b)). Most records (N=32) cover the last several thousand up to about 10 kyr BP while only a few records cover several tens of thousands of years (e.g. #8 to #10). Likewise, the time periods covered do vary either

https://doi.org/10.5194/cp-2022-96
Preprint. Discussion started: 24 January 2023


Climate of the Past Discussions

due to the availability of lake sediments, diatom abundances in a lake and/or scientific foci of the research groups. By far the highest number of records is available for MIS 1 (N=37) and especially for the last 2 kyrs (N=48). MIS 2 is still covered by 19 records, whereas towards MIS 3 (N=5) and beyond fewer records have been generated. However, single records cover even time periods in MIS 11 (at Lake Baikal; #2) and beyond (MIS G1/104, #1), outlining the applicability of this proxy across a wide range of time scales. A paleo lake from the Baringo–Bogoria Basin (record #1), is the oldest lacustrine $\delta^{18}O_{BSi}$ record and has been dated to the onset of MIS 104 in the late Pliocene (Wilson et al., 2014b).

Regarding the number of published records by continent (Fig. 3), there is a clear focus on Asia and Europe with 21 and 15 records published, respectively. In Asia, there is a strong regional focus on Siberia, whereas most other parts of the continent are not yet investigated for lake sediment $\delta^{18}O_{BSi}$. A regional focus also occurs in Africa and South America. While a sizeable number of records stemming from these continents have been published (N=10 and N=11, respectively), there are pronounced regional foci in the East African Rift and the Andes, respectively. Another focus region is Alaska, where most (N=6) of the published North American records (N=7) are located. $\delta^{18}O_{BSi}$ work has also been carried out in Oceania with published records from lakes in New Zealand (#42) and South Georgia (#19).

In summary, the distribution of available $\delta^{18}O_{BSi}$ data displays, thus, a bias towards the mid– to high latitudes of the northern hemisphere. Additionally, this distribution is also indicative of the site accessibility and (regional) research foci of the working groups. This has a rather pronounced effect on the spatial distribution of available $\delta^{18}O_{BSi}$ records. The geographical distribution is also indicative of cold regions devoid of carbonates where biogenic silica is the most promising archive to obtain oxygen isotope records from lake sediments.

This pattern also affects the latitudinal distribution of the records (see also Tab. A1) with records ranging from 54.17 °S (# 19) to 69° N (# 39). Records stemming from low–latitude lakes (particularly in Africa and South America) are often located at high altitudes above 3000 m asl (above sea level; e.g., #11, 17, 18, 21). Lake Simba Tarn (record #34) features the maximum altitude for an individual $\delta^{18}O_{BSi}$ record of 4959 m asl. Altitudes below 1000 m asl, however, are most common (N=36), especially for high–latitude lakes. In total, 12 lakes are located below 100 meters asl (e.g., #29, 35). Many of these low–altitude lakes are located in maritime locations in immediate proximity to the coast (e.g., #19, 30) or have even had marine intrusion stages in the past (a postglacial transgression at Nettilling Lake; #41). Extremely continental environments are tackled in central and eastern Siberia and the Lake Baikal region (e.g., #4, 8, 9, 10, 25).

https://doi.org/10.5194/cp-2022-96
Preprint. Discussion started: 24 January 2023

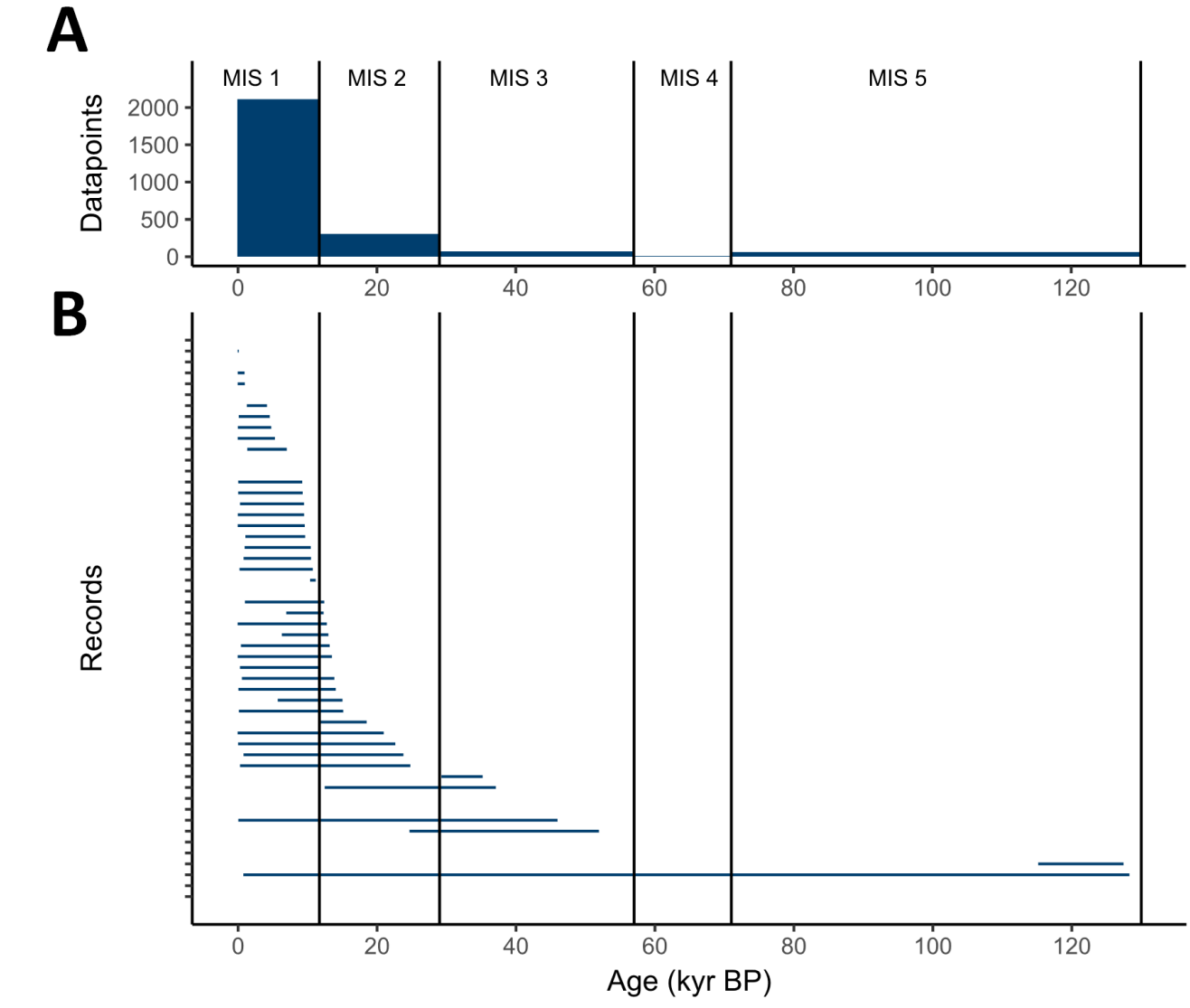

320 **Figure 2. Temporal coverage by records and datapoints during MIS 1 – MIS 5. a) Total number of datapoints available during each Marine Isotope Stage. b) Temporal coverage of records.**

325

https://doi.org/10.5194/cp-2022-96
Preprint. Discussion started: 24 January 2023

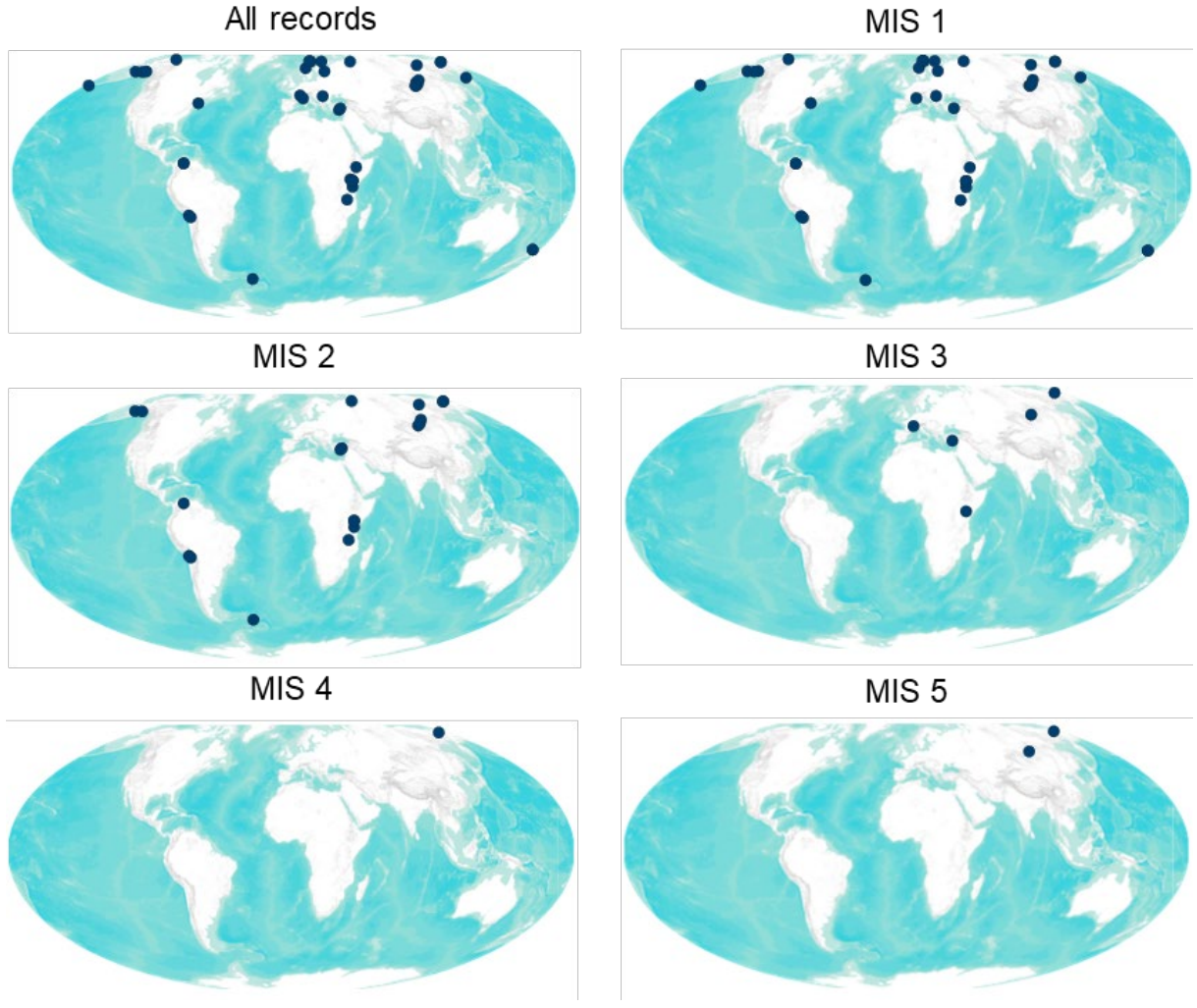

Figure 3. World map depicting the locations of $\delta^{18}O_{BSi}$ records with chronology. Note that one location may correspond to more than one records. ©ESRI 2022

3.3 Spatial coverage and resolution of combined records

Varying spatial resolution among the compiled isotope records is linked to the fact that lakes and their corresponding catchments are not points in space but areas. Consequently, lake water and, thus, the related $\delta^{18}O_{BSi}$–signal represent a spatial average, integrating over the catchment size of the respective lake. Lake basin sizes range from small ponds of <1 km² (e.g. #19, 11, 23, 33, 34) to some of the largest lakes in the world, including lake Malawi and Lake Baikal covering 29,544 km² and 31,968 km², respectively (Fig. 4A). Large and voluminous lakes are the exception, however, and most of the lakes represented here are <10 km² in size (N=25). Note that in case of paleo lakes, such parameters are not applicable. While authors sometimes provide estimates on paleo lake extent, these figures are not consistent with the values determined for present lakes and are

https://doi.org/10.5194/cp-2022-96
Preprint. Discussion started: 24 January 2023

Climate of the Past Discussions

therefore not included in the evaluation of the dataset. Catchment sizes vary by several orders of magnitude as well. For small lakes, catchments are often <10 km² (N=13, e.g. #22, 33, 37), whereas the largest lakes, Lake Malawi and Lake Baikal feature catchments of 128,727 km² and 569,176 km², respectively (Fig. 4A). Therefore, these lakes integrate the environmental signal over a large and potentially diverse region in terms of hydrology. While most of the lakes compiled in this study are primarily fed by surface runoff and/or precipitation (according to the original publications of records), groundwater influx may also play a pivotal role. Groundwater influx may introduce a large memory effect of past precipitation due to the generally long residence times of aquifers. This may have an impact on records especially when looking at short timescales. Groundwater input, however, is usually not accounted for and, thus, beyond the scope of our study. In summary, both lake sizes and catchment sizes vary by several orders of magnitude (Fig. 4A) among the sites with existing $\delta^{18}O_{BSi}$ records, and span from local signals to regional averages. However, most of the records (N=18) stem from lakes with catchments <100 km², suggesting rather local signals. While single local signals represent small areas, different local signals may well correlate on continental and hemispheric scales.

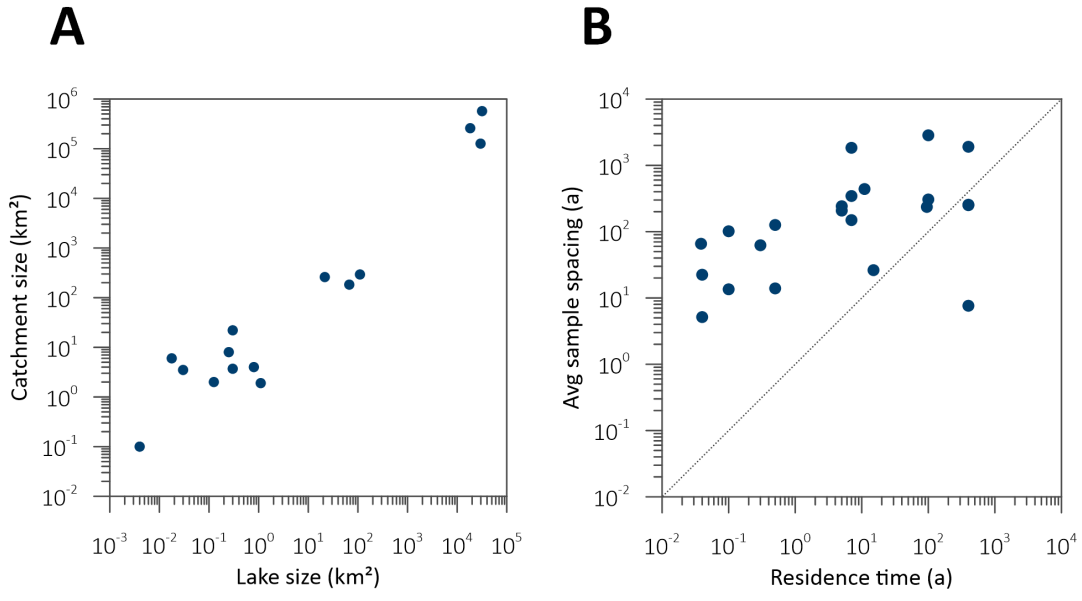

Figure 4. A) Depiction of corresponding lake and catchment sizes of the records compiled within this study. One lake may correspond to more than one records. Note that records from Paleo-lakes and lakes with incomplete information on lake and catchment size were not considered for this figure (N=33). B) Depiction of corresponding sampling intervals and t_{res}. Note that records from lakes without information on t_{res} were not considered for this figure (N=37).

3.4 Temporal coverage and resolution of combined records

Temporal resolution of the records and the resulting signal properties are determined by both the lake basin itself (i.e. accumulation rates and preservation of diatom silica) and the sampling routine applied to the sediment core (i.e. the

https://doi.org/10.5194/cp-2022-96
Preprint. Discussion started: 24 January 2023


Climate of the Past Discussions

sampled intervals as well as the thickness of individual samples). Data on the thickness of single sediment samples taken from the cores are, however, scarce in the original publications. The same applies for information on the time interval or number of years represented by a single sediment sample. Consequently this parameter and its potential effect on the records' signal properties could not be investigated in detail in this manuscript. We therefore focus on t_{res} and sampling frequency of a core as a means of characterizing the records and their temporal resolution.

The t_{res} is closely linked to the size of lake basins and varies accordingly. It ranges from several weeks for small lakes (e.g., #49, 50) to centuries (219 and 375 years for Lake Malawi and Lake Baikal, respectively). On the whole, t_{res} of sub–annual to annual scale are most common (N=17) among the lakes considered in this study (Fig. 4B). It should be noted that longer t_{res} leads to averaging of the signal over a longer time period. Likewise, different t_{res} may also have an effect on absolute $\delta^{18}O_{BSi}$ values and variabilities. Lakes with very long t_{res} (t_{res}>100 years) are tendentially more susceptible to lake evaporation, and may effectively behave like closed–system lakes with regard to the $\delta^{18}O_{BSi}$ signal even if they are hydrologically open (i.e. have outflows). These are still referred to as hydrologically open in this work and hydrological settings and t_{res} are addressed separately in the discussion.

Also the sampling frequency varies by several orders of magnitude (Fig. 4B). It stretches from annual to multi–millenial timescales. Consequently, the signal properties and the recorded climatic and/or hydrological forcings of the identified records can be expected to vary accordingly. Most records, however, plot in the top left half of graph of Fig. 4B, which indicates that the temporal offset between two sediment samples exceeds t_{res}. This suggests that the sampling routine is the limiting factor of the temporal resolution of these records. Only three records from Lake Baikal plot in the lower right half of Fig. 4B, suggesting in these cases (#4, #20, #51) t_{res} to be the dominant factor in determining the record's resolution, at least with respect to inflow–related changes.

We thus conclude that the sampling resolution is the main factor determining the temporal resolution of most records with t_{res} acting as an additional smoothing mechanism. A lake with a centennial–scale t_{res} can, therefore, display centennial–scale changes of climate and hydrology to their full amplitude. Decadal–scale changes, on the other hand, can be expected to be attenuated by an order of magnitude in a lake with centennial–scale t_{res}. Based on t_{res} and sampling resolutions of the records, comparing records on a centennial or millennial scale is the most promising approach for assessing common patterns.

4 Discussion

4.1 Common Era Climate

The Common Era subset of records including only records stemming from sites north of 45° N (Fig. 5A, N=19), comprises 460 datapoints. The records display considerable offsets with $\delta^{18}O_{BSi}$ values ranging from +19‰ (#34) to +33‰ VSMOW (#35). These offsets can be linked to their individual environmental setting, e.g. latitudinal and continentality effects, as well as to their potential to be prone for lake evaporation. Amplitudes in $\delta^{18}O_{BSi}$ of these records vary from 0.4‰ (#24) to circa 9‰

https://doi.org/10.5194/cp-2022-96
Preprint. Discussion started: 24 January 2023


Climate of the Past Discussions

VSMOW (#35). This variability might correspond to their different hydrological settings. Closed lakes (such as Sunken Island Lake; #26) have a tendency towards higher $\delta^{18}O_{BSi}$ amplitude likely due to lake evaporation leading to a more enriched isotope signature in the lake (Broadman et al., 2020b).

Binned records (Fig. 5B, N=14) do not display any common pattern and feature $\delta^{18}O_{BSi}$–values ranging from +20‰ to +31‰ VSMOW. However, binning of datapoints and exclusion of shorter records reduces the $\delta^{18}O_{BSi}$ amplitudes of individual records, to less than 5‰. Offsets between individual records may be linked to site–specific characteristics of individual lakes and catchments, as well as latitudinal and continentality effects.

After mean removal (Fig. 5C) the CE data suggest a common trend with high $\delta^{18}O_{BSi}$ values at 1900 yrs BP and a general decrease until the present with the lowest values occurring in the last two bins (or 400 years). Some records also show maxima between 500 and 1100 yrs BP and minima at ca. 1300 yrs BP. The subsets for hydrologically open lakes (N=13, Fig. 5D) and hydrologically open lakes with t_{res}<100yrs (N=9, Fig. 5E) show a similar picture.

The combined Common Era records (Fig. 5F) comprise 8 records and show a general $\delta^{18}O_{BSi}$ decrease over the last 2 kyr amounting to ca. 2‰ VSMOW. The $\delta^{18}O_{BSi}$ amplitude within individual bins, however, might exceed this number, most notably at 100, 1300 and 1900 yrs BP, which show the highest amplitudes of up to 5‰ for the Common Era. This is in line with differences between the timing of $\delta^{18}O_{BSi}$ maxima and minima between North American and Eurasian records. At centennial scale, these differences might also be linked to dating uncertainties. Moreover, the record of Lake Bolshoye Shchuchye (#16) features a much larger amplitude. Its exceptional $\delta^{18}O_{BSi}$ variability has been attributed by the authors to variations of snow and snow melt in the lake's catchment and therefore does represent a different kind of precipitation–based signal compared to most other records. The combined trend features its highest $\delta^{18}O_{BSi}$ values at 1900 yrs BP, followed by a decrease leading to a relative minimum at 1100 and 1300 yrs BP. This phase is followed by a second $\delta^{18}O_{BSi}$ peak at 700 and 900 yrs BP, after which a decrease can be observed. The decrease at 300 and 500 yrs BP features the least deviation between individual records. The most recent bin shows again a much larger $\delta^{18}O_{BSi}$ variability. While most records display the lowest values at this time, Lake Kotokel (#8) for instance shows an increase compared to the previous bins. This increase may or may not be related to recent warming; and due to the complex hydrology of the lake even lake evaporation cannot be ruled out. The majority of the records however does not indicate a recent $\delta^{18}O_{BSi}$ maximum, indicative for any impact of recent warming. It has to be noted that there is bias of data points towards the older end of the most recent bin. An absence of recent warming in

https://doi.org/10.5194/cp-2022-96
Preprint. Discussion started: 24 January 2023

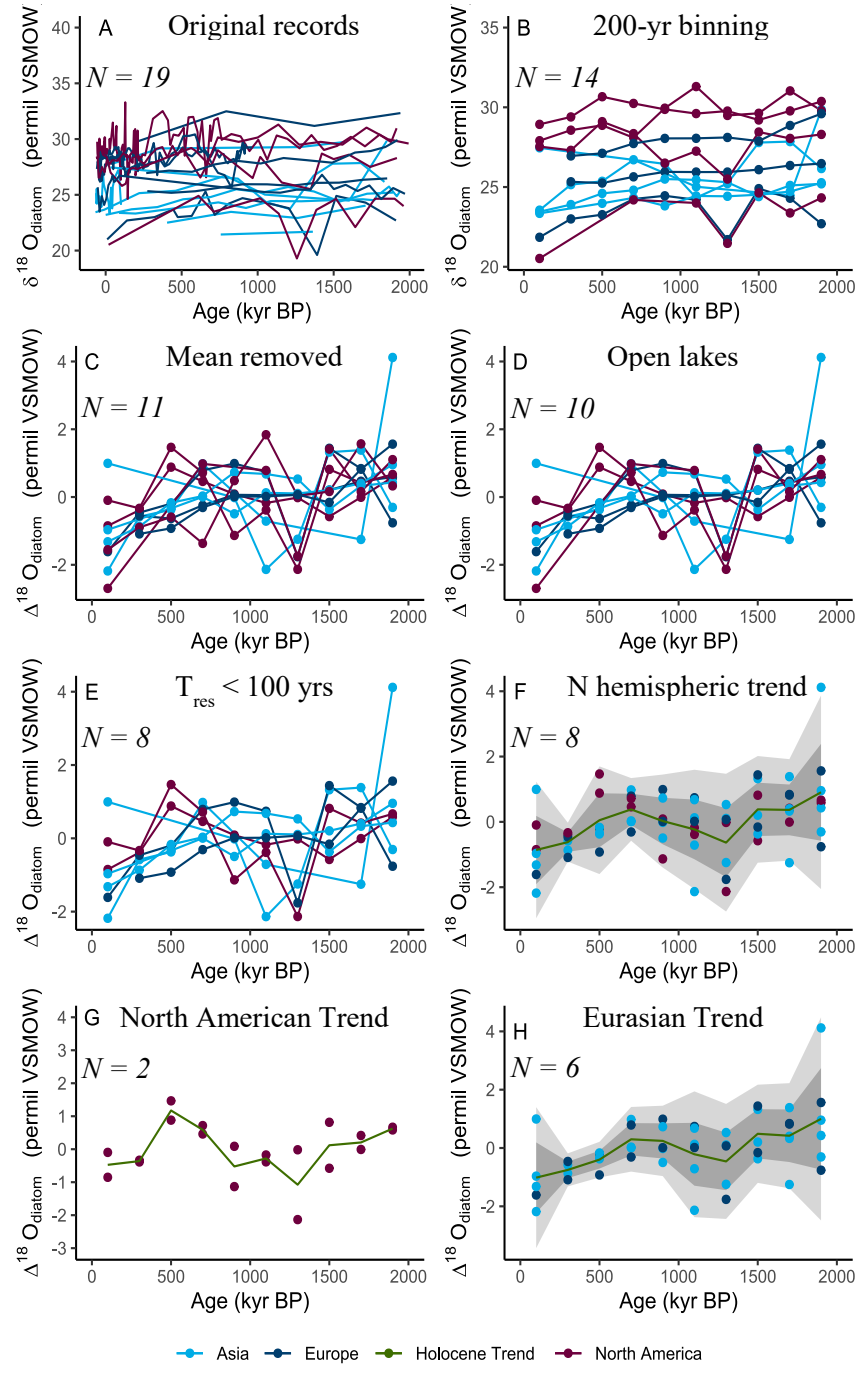

Figure 5. Common Era Northern hemispheric records (45-90 N) compiled in this study. A) Original records, B) data binned to 200 year intervals, only showing records covering at least 7 bins, C) binned records with mean of individual records removed, D) filtered for records from open lakes only, E) filtered for records from lakes with t_{res}<100 yrs, F) NH trend, calculated as mean of all records in each bin. Shadings show 1 and 2 standard deviations, respectively. G) North American and H) Eurasian trend.

https://doi.org/10.5194/cp-2022-96
Preprint. Discussion started: 24 January 2023


Climate of the Past Discussions

the data therefore might be linked to this bias and does not rule out a reaction of lake systems to recent warming. As Eurasian records constitute the majority of records (N=7), the Eurasian trend is similar to the NH picture (Fig. 5H).

North American records (N=2) do not show a consistently decreasing trend (Fig. 5G), but slightly higher values at 1700 and 1900 yrs BP compared to the most recent bins (100 and 300 yrs BP, respectively). They do, however, show lower $\delta^{18}O_{BSi}$ values between 900 and 1300 yrs BP, followed by a $\delta^{18}O_{BSi}$ maximum at 500 yrs BP. As there are only two records available after filtering, caution has to be applied in interpreting this pattern.

Common patterns among Eurasian, and possibly NH, $\delta^{18}O_{BSi}$ records do suggest a common NH signal throughout the Common Era. The observed maxima and minima correspond to previously described climatic events, notably the Roman Warm Period from 2000 yrs BP to about 1600 yrs BP (Ljungqvist, 2010), the Dark Ages Cold Period from 1600 to 1200 yrs BP (Büntgen et al., 2016; Helama et al., 2017) the Medieval Climatic Anomaly (MCA) from 1200 yrs BP to 800 yrs BP (Bradley et al., 2003; Mann et al., 2009) and the Little Ice Age from 700 yrs BP to 100 yrs BP (Matthews and Briffa, 2005). The good accordance of our data with these previously described warm and cold phases suggests that $\delta^{18}O_{BSi}$ records presented are influenced by T_{air} change, either directly or via other parameters which are linked to T_{air}. Recent research has rejected the global nature of these climatic events and suggested that they are regionally constrained (Neukom et al., 2019). However, the accordance of our data – when assessed at centennial scale – with these climatic events makes sense because they were initially described for North America and Europe.

4.2 Holocene (corresponding to MIS 1) Climate

The Holocene NH subset of records consists of 21 records which display considerable offsets of their mean $\delta^{18}O_{BSi}$ values ranging from +20‰ (#3) to +35‰ (#31) VSMOW (Fig. 6A). Lake El'gygytgyn (#3) is located in a continental, high–latitude environment with little secondary evaporation (Chapligin et al., 2012b) whereas Lake Ladoga (#31) is situated in a less continental, lower latitude setting with a complex hydrological history of changing inflows and outflows (Kostrova et al., 2019).

Amplitudes of the individual Holocene records vary from less than 5‰ (#3) to circa 10‰ VSMOW (#20, #35). Lake El'gygytgyn (#3) is a voluminous, deep hydrologically open lake with little lake evaporation, whereas Heart Lake (#35) is a much smaller, less voluminous lake. Lake Baikal (#20) is a deep voluminous lake like Lake El'gygytgyn, however with a centennial–scale t_{res} making it effectively closed and thus potentially subject to secondary evaporation. Consequently, differences in their isotopic variability might correspond to their different hydrological settings. Closed lakes (such as Sunken Island Lake; #26) have a tendency towards higher $\delta^{18}O_{BSi}$ amplitude likely due lake evaporation leading to a more enriched isotope signature of lake water (Broadman et al., 2020b).

https://doi.org/10.5194/cp-2022-96
Preprint. Discussion started: 24 January 2023

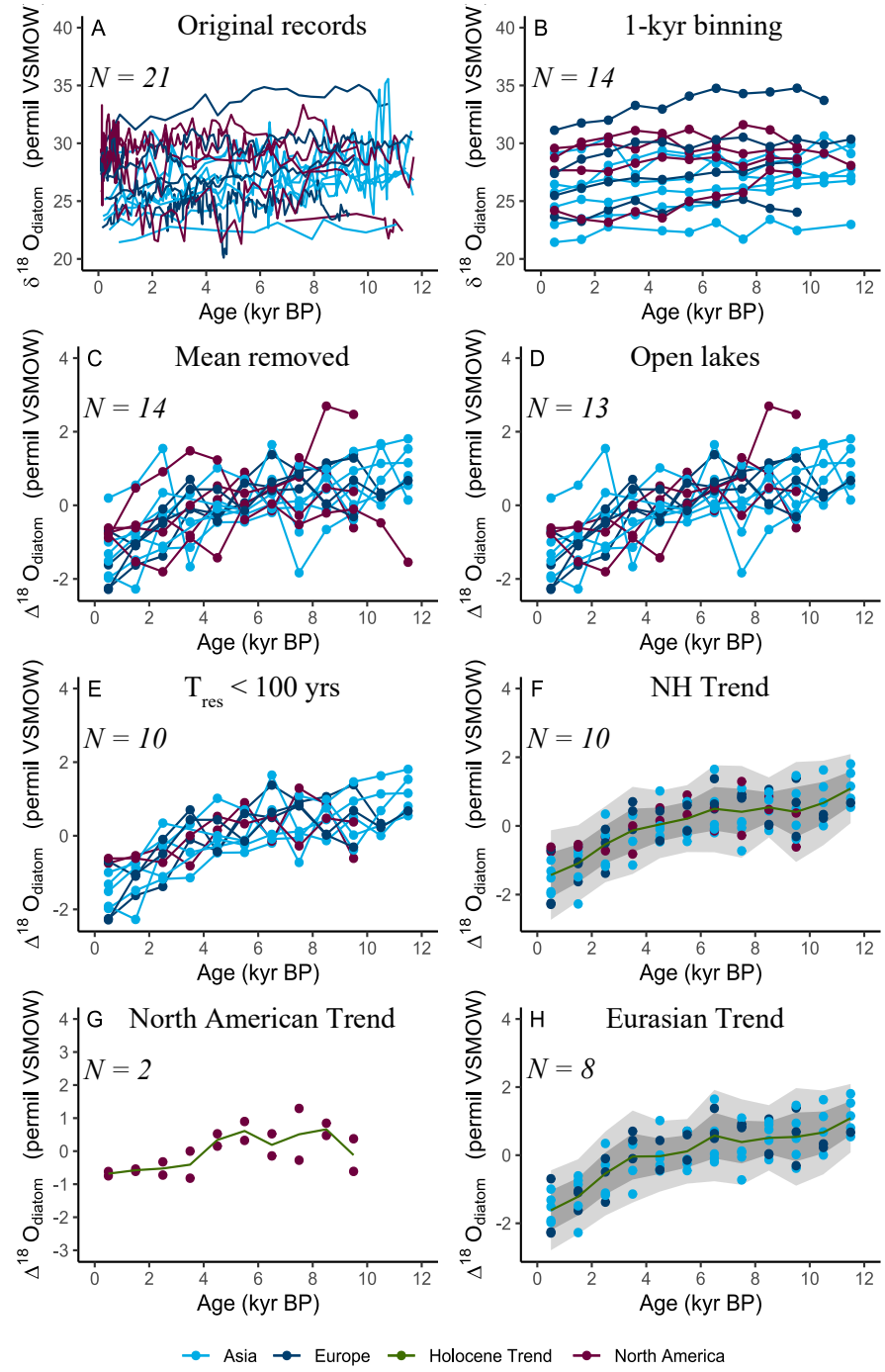

Figure 6. MIS1 Northern hemispheric records (45-90 N) compiled in this study. A) Original records, B) data binned to 1-kyr intervals, only showing records covering at least 7 bins, C) binned records with mean of individual records removed, D) filtered for records from open lakes only, E) filtered for records from lakes with t_{res}<100 yrs, F) NH trend, calculated as mean of all records in each bin. Shadings show 1 and 2 standard deviations, respectively. G) North American and H) Eurasian trend.

https://doi.org/10.5194/cp-2022-96
Preprint. Discussion started: 24 January 2023


Climate of the Past Discussions

Binned records (Fig. 6B, N=14) do not display any common pattern and feature $\delta^{18}O_{BSi}$–values ranging from +20‰ to +35‰ VSMOW, similar to the original records. However, binning of datapoints and exclusion of shorter records results in smoothed amplitudes of less than 5‰ VSMOW. Early Holocene binned records seem to have $\delta^{18}O_{BSi}$ values (up to 2.5‰) higher than the Holocene mean, whereas late Holocene values are generally up to 2‰ below the Holocene mean. However, some records do not follow this general pattern after mean removal (Fig. 6C). This could be indicative of the fact that the dataset still features lakes with different hydrological settings and t_{res} which have a substantial impact on the recorded signal.

Filtering for hydrologically open lakes (Fig. 6D, N=13) and t_{res}<100 yrs (Fig. 6E, N=10) displays a clear decreasing $\delta^{18}O_{BSi}$ trend of 2.5‰ throughout the Holocene. Differences between individual records do exist, though. Most notably, the absolute $\delta^{18}O_{BSi}$ maxima of individual records do not occur at the same time. While some records feature maxima at the beginning of the Holocene, other records feature maxima between 5 and 8 kyr BP. This pattern is in line with Holocene T_{air} reconstructions which have found spatial differences of the timing of the Holocene thermal maximum (Kaufman et al., 2004; Renssen et al., 2009).

Based on this subset of hydrologically open lakes with t_{res}<100 yrs, a combined millennial scale NH trend was calculated. This combined Holocene trend (Fig. 6F) shows a decrease throughout the Holocene amounting to ca. 2‰ VSMOW. The absolute maximum is observed for the Early Holocene bin at 11–12 kyr BP. A decrease at the beginning of the Holocene between 12 kyr BP and 10 kyr BP is followed by a relatively stable middle Holocene until 6 kyr BP and subsequent stronger decrease towards the absolute $\delta^{18}O_{BSi}$ minimum in the youngest bin (0–1 kyr BP).

When considered separately, North American (N=2) and Eurasian (N=8) records show different patterns and have been described and interpreted differently in the case studies published to date. While the former are primarily liked to atmospheric circulation changes in Alaska (Bailey et al., 2018; Broadman et al., 2020b; Broadman et al., 2020a), the latter are at least partly interpreted as indicative of T_{air} and insolation changes (Swann et al., 2010; Mackay et al., 2011; Chapligin et al., 2012b; Kostrova et al., 2013a; Kostrova et al., 2019; Kostrova et al., 2021). Eurasian $\delta^{18}O_{BSi}$ records (N=8) display a slight decrease from 12 kyr BP to 10 kyr BP and suggest a second maximum at 7 kyr BP followed by a second relatively stable phase. An accelerated decrease starting at ca. 4 kyr BP constitutes a more abrupt change than in the NH trend. North American records do not show a consistently decreasing trend throughout Holocene (Fig. 6G), but rather slightly higher $\Delta^{18}O_{BSi}$ values in the first half of the Holocene as compared to the second half. Since there are only two North American records fulfilling the aforementioned criteria, it is difficult to meaningfully go beyond the existing case studies, outlining the necessity for further research in this region.

The regional differences between North America and Eurasia are also manifested in the timing of absolute $\delta^{18}O_{BSi}$ minima and maxima of individual records (Fig. 7). The spatial pattern of the Holocene maxima of binned records shows a different timing of maxima for different regions (Fig. 7). Eastern Eurasian sites feature a pronounced early Holocene maximum (at 12 kyr BP), whereas sites more to the west of Eurasia show tendentially rather a middle Holocene maximum, around 6–8 kyr BP. This suggests that the double maxima of the Eurasian trend (Fig. 6H) is at least partly caused by the regional differences over

https://doi.org/10.5194/cp-2022-96
Preprint. Discussion started: 24 January 2023

Climate of the Past Discussions

Eurasia. There are also individual records, however, which do show two peaks within the Holocene e.g. Lake Bolshoye Shchuchye from the Polar Ural Mountains (#16). Records from Alaska feature later $\delta^{18}O_{BSi}$ maxima (5 kyr BP and 7 kyr BP, respectively).

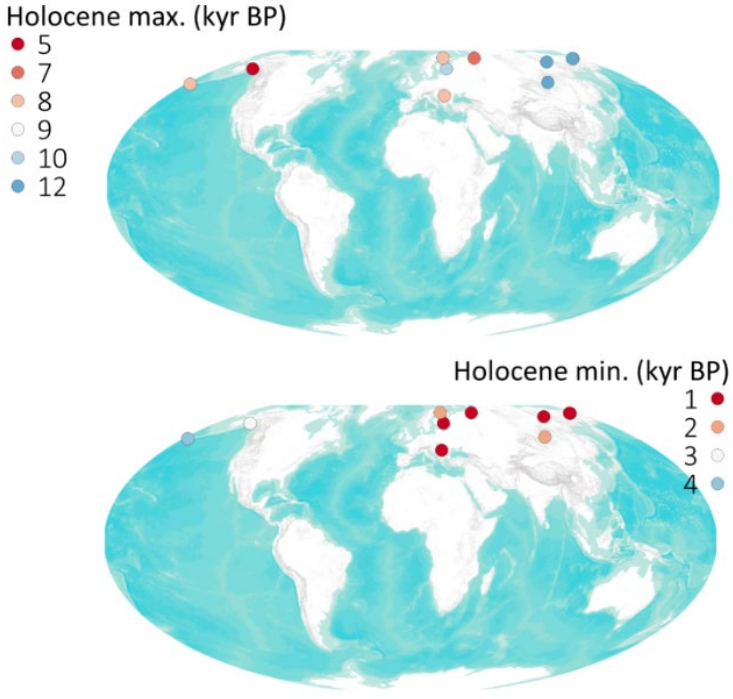

Figure 7. Timing of maxima and minima of binned records in the Holocene. Filter criteria are the same as indicated in Fig. 10 and only records covering at least 10 bins have been considered. ©ESRI 2022

The timing of Holocene minima is rather homogenous in northern Eurasia with all records reaching their minimum in the last 1 kyr BP or between 1 kyr BP and 2 kyr BP (Fig. 7). While the records generally follow the same decreasing long–term $\delta^{18}O_{BSi}$ trend, they feature either early or late Holocene minima. Since datapoints of 1850 CE and younger have been removed from the dataset prior to analysis to exclude the industrial era, a potential effect of recent climate change is not covered in this subset of data. As with the Holocene maximum, sites in Alaska also differ with regard to Holocene minimum. They tendentially show absolute minima earlier than Eurasian records (3 and 4 kyr BP, respectively). This underlines once more, the different behaviour of the regions (North America and Eurasia).

https://doi.org/10.5194/cp-2022-96
Preprint. Discussion started: 24 January 2023


Climate of the Past Discussions

4.3 Combined Holocene trend in the hemispheric context

The combined trends of $\delta^{18}O_{BSi}$ for NH, Eurasia and North America are shown in comparison to other NH proxy records in Fig. 8. As individual $\delta^{18}O_{BSi}$ records are commonly discussed with respect to insolation, we provide June and December insolation curves for 60°N, calculated using (Laskar et al., 2004). As visible in Fig. 8, Eurasian and NH combined trends show a similarity with the June insolation as all records feature a decreasing trend throughout the Holocene. However, insolation decreases steadily after an early Holocene maximum whereas combined NH and Eurasian $\delta^{18}O_{BSi}$ trends feature a stable early Holocene and a second peak at 7 kyr BP. This presumably relates to the geographical distribution of the timing of $\delta^{18}O_{BSi}$ maxima and minima as discussed above. Therefore, eastern Eurasian records are most in line with June insolation which has been regarded as a proxy of summer T_{air}. Records stemming from sites further west are less directly correlated with June insolation. A striking difference is the accelerated decrease of $\delta^{18}O_{BSi}$ after 4 ka, co-incident with neo-glacial-cooling which is not mirrored in the insolation curve. The relatively stable insolation during this time suggests that the accelerated decrease visible in $\delta^{18}O_{BSi}$ records must be driven by other factors.

Conversely, December insolation shows an anticorrelation with the $\delta^{18}O_{BSi}$ records. However, as both the absolute values and the changes in December insolation are an order of magnitude lower than those of June insolation, a decisive influence of December insolation on $\delta^{18}O_{BSi}$ records can be ruled out. This is in good agreement with previous works, claiming that the $\delta^{18}O_{BSi}$ proxy yields a summer–dominated signal (Shemesh et al., 2001a; Kostrova et al., 2021). It has to be noted that the records displayed still stem from different latitudes and the insolation patterns are not identical at all these sites. A decrease of summer insolation, however, is generally the case for high latitude regions throughout the Holocene.

https://doi.org/10.5194/cp-2022-96
Preprint. Discussion started: 24 January 2023

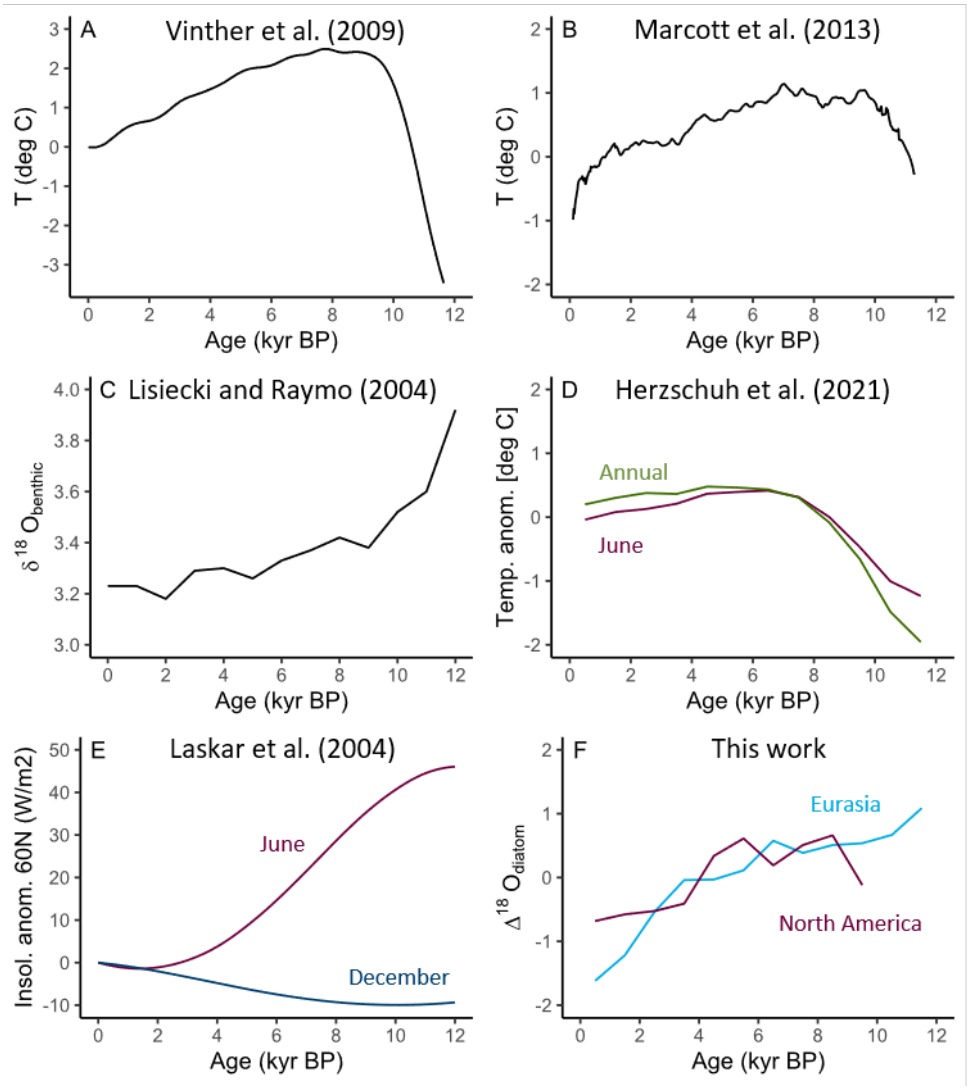

Figure 8. Combined Trend of δ18OBSi compared to other climate reconstructions. A) Greenland ice sheet temperature reconstruction, B) Multi-proxy temperature reconstruction (30-90 N), C) global stack of δ18O from benthic foraminifera, D) temperature reconstruction (45-90 N) based on pollen data, E) Insolation anomaly for June and December, F) Combined Eurasian and North American Trend from δ18OBSi records (this work).

Temperature reconstructions by Vinther et al. (2009) using $\delta^{18}O$ data from ice cores at Agassiz ice cap and Greenland (between 65°N and 80°N) show a pronounced T_{air} increase of about 5°C at the beginning of the Holocene until 10 kyr BP, followed by a stable phase until 7 kyr BP. While the NH and Eurasian trends do not feature this increase during the early Holocene, they do show a relatively stable phase from 10 kyr BP to 7 kyr BP. After 7 kyr BP, both the NH $\delta^{18}O_{BSi}$ trend and the NH T_{air} reconstruction feature a decrease of circa 2°C and 1.5‰ VSMOW, respectively. As the present–day global average T_{air}–dependent fractionation in precipitation amounts to 0.695‰/°C (Dansgaard, 1964), a 1.5‰ $\delta^{18}O$ decrease would, thus,

https://doi.org/10.5194/cp-2022-96
Preprint. Discussion started: 24 January 2023


Climate of the Past Discussions

correspond to a 2°C cooling, the same T_{air}–change as found by Vinther et al. (2009). This good agreement of $\delta^{18}O_{BSi}$ combined trends (NH and Eurasia) and the T_{air}–reconstructions by Vinther et al. (2009) suggests summer T_{air} to have a major impact on $\delta^{18}O_{BSi}$ records on millennial time scales.

Multi–proxy–based temperature reconstructions by Marcott et al. (2013) (regional stack 30°N to 90°N) also show a temperature increase until 10 kyr BP, followed by a stable phase until ca. 7 kyr BP and a decrease of ca. 2°C thereafter. This temperature reconstruction includes a much broader geographical focus as well as different archives. Thus, the stable phase from 10 kyr BP to 7 kyr BP and a maximum around 7 kyr BP are shared features of the $\delta^{18}O_{BSi}$ trends of this work, the ice core reconstruction from Vinther et al. (2009) and the temperature reconstructions by Marcott et al. (2013). However, the early Holocene maximum of the $\delta^{18}O_{BSi}$ trends is not represented in reconstructions by Vinther et al. (2009) and Marcott et al. (2013). This discrepancy might reflect different regional biases of Marcott et al. (2013) and this work, which is also in line with the different timing of Holocene maxima in the $\delta^{18}O_{BSi}$ data (Fig. 8). Additionally, it might also indicate other influences than T_{air} on the $\delta^{18}O_{BSi}$ signal in the frame of a more complex climate system during the early Holocene. Given the discrepancy between temperature reconstructions and $\delta^{18}O_{BSi}$ records in the early Holocene, it is likely that the influence of factors other than T_{air} is especially pronounced in the early Holocene. The LR04 stack of the $\delta^{18}O$ of benthic foraminifera (Lisiecki and Raymo, 2005) features continuously decreasing $\delta^{18}O$ throughout the Holocene which is in accordance with the combined Eurasian $\delta^{18}O_{BSi}$ trend.

Pollen records may help to further investigate this issue as they stem from terrestrial environments, often even also from lake sediments. Moreover, they offer a similar temporal and geographical focus compared to our records, extending to high latitudes. For this comparison we have used a pollen data compilation by Herzschuh (2021) comprising data from 864 records from sites north of 45°N for the Holocene. Changes of annual T_{air} and July T_{air} relative to modern values were retrieved from the pollen dataset. Annual and July T_{air} show similar patterns with a pronounced early Holocene increase, followed by middle Holocene maximum and a less pronounced decrease until the present day. Both the middle Holocene maximum and the subsequent decrease of T_{air} are in good agreement with the combined Eurasian $\delta^{18}O_{BSi}$ trend (Fig. 8A, 8D). This further supports a substantial influence of T_{air} on the $\delta^{18}O_{BSi}$ signal. However, the early Holocene maximum of $\delta^{18}O_{BSi}$ in our combined NH and Eurasian trends is not reflected by pollen–based reconstructions. Caution has to be applied when using pollen–based climate reconstructions for comparison because vegetation changes may lag behind changes of climatic variables (Herzschuh et al., 2016). In summary, the similarity of our combined $\delta^{18}O_{BSi}$ trends with NH temperature reconstructions and insolation data allows for deducing a clear link to summer T_{air} for the Holocene records.

It has to be stressed that this influence of T_{air} may act both directly and indirectly. Directly by means of the temperature–dependent fractionation during precipitation formation, and indirectly via the impact of temperature on the hydrological cycle and $\delta^{18}O$ of water compartments. This includes factors such as moisture origin, precipitation intermittency and atmospheric circulation patterns which have been described as key drivers in numerous case studies. This underlines the importance of scale when assessing $\delta^{18}O_{BSi}$ records, both temporally and spatially. On a millennial and hemispheric scale, T_{air} can be identified as one main driver of $\delta^{18}O_{BSi}$ records even though the signal formation is generally complex and challenging to interpret with

https://doi.org/10.5194/cp-2022-96
Preprint. Discussion started: 24 January 2023

individual records. A T_{air} influence for certain records on the millennial scale is therefore not necessarily a contradiction to the findings of the original publications which may have attributed the record's signal to other factors (e.g., hydrological processes) on shorter timescales.

4.4 Frontiers and Challenges (Records older than MIS 1)

Further back in time than MIS 1, coverage with $\delta^{18}O_{BSi}$ records is generally limited. As MIS 1 (N=37) and MIS 2 (N=18) have the highest numbers of records, they offer the best possibility of comparing glacial and interglacial records. Records beyond MIS 2 are very sparse and do not allow for filtering and generating common trends. Here, the interpretation has to rely on comparison of individual datasets. There are few (N=16) records only which cross the MIS 1–MIS 2 boundary and these records cover neither MIS 1 nor MIS 2 entirely. A quantitative comparison of MIS 1 and MIS 2 is therefore difficult. Again, caution has to be applied due to the fact that these records stem from lakes with different hydrological and climatic settings (i.e. maritime Alaskan sites vs. continental Siberian sites).

The most promising approach for investigating MIS 1 and MIS 2 is extending the NH MIS 1 datasets to the past (Fig. 9). Five NH $\delta^{18}O_{BSi}$ records (#3,8,15,24,25) extend back from MIS 1 into MIS 2 and offer insight into the hydroclimate history of Siberia during the last glacial and the deglaciation. Most of these records display a maximum near the MIS 1–MIS 2 boundary and a decrease of $\delta^{18}O_{BSi}$ with increasing age in MIS 2, suggesting decreasing T_{air}. This is the case for all records except #3 which displays a relative $\delta^{18}O_{BSi}$ maximum at ca. 16 kyr BP. This maximum may also be caused by dry conditions outperforming the effect of lower T_{air}. Only records #3, #8 and #15 extend beyond 13 kyr BP. Both #3 and #15 reach their absolute minima at 23 kyr BP and 24 kyr BP, respectively. Record #8 does not show such a clear pattern and shows a relative maximum at 25 kyr BP instead. This is likely due to the complex hydrological setting (alternating between open and closed at present) which may have changed over these timescales. Generally, most records suggest a lower $\delta^{18}O_{BSi}$ in MIS 2 when compared to MIS 1.

This is remarkable as glacial and interglacial periods feature different environments, atmospheric circulation patterns and likely hydrological settings (e.g. formation or closure of outflows from lakes, lake level fluctuations). Potentially, lower $\delta^{18}O_{BSi}$ values would be conform with either lower T_{air} or more humid conditions. In case of MIS2, generally associated with cold and dry conditions, a lower T_{air} is the more plausible scenario.

Considering all records covering the MIS 1–MIS 2 boundary, without geographical or hydrological constraints, yields a less clear picture (Fig. 9). The calculated offsets of MIS 1 and MIS 2 datapoints may show both higher and lower $\delta^{18}O_{BSi}$ values in MIS 2 compared to MIS 1. Again, an MIS 2 climate colder and drier than Holocene (MIS 1) may produce either lower or higher $\delta^{18}O_{BSi}$ values due to opposing effects of T_{air} and evaporation. A geographical pattern of either of these effects prevailing is not obvious, which suggests that rather than the climatic background, the individual hydrological settings of the lakes in question play a prominent role in determining the $\delta^{18}O_{BSi}$ signal. This supports the approach of using lakes with both similar latitudinal and hydrological characteristics.

https://doi.org/10.5194/cp-2022-96
Preprint. Discussion started: 24 January 2023

Climate of the Past Discussions

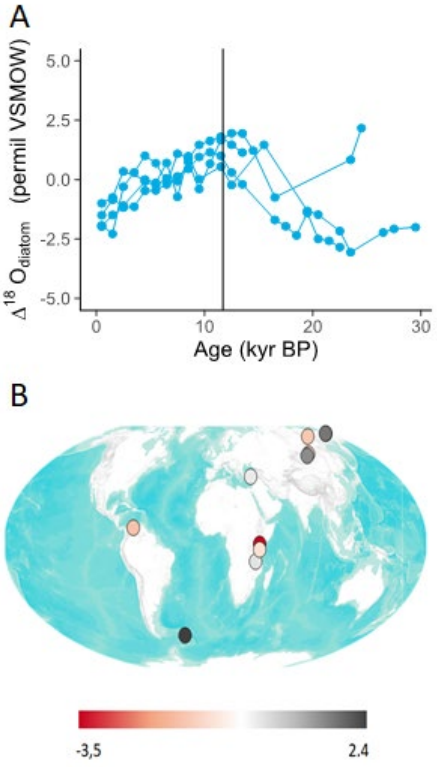

Figure 9. Comparison of MIS 1 and MIS 2 data. a) continuation of records from NH Stack (see Fig. 6F) into MIS 2. b) Difference between MIS 1 and MIS 2 means of all individual records covering the MIS 1 – MIS 2 boundary. ©ESRI 2022

Further back in time than MIS 2, records become even scarcer, as do lake sediments in general. Additionally, lake sediments covering these time periods often lack sufficient diatoms, especially in cold stages, i.e. Lake Baikal during MIS 4 (Mackay et al., 2008; Mackay et al., 2011; Mackay et al., 2013).

Lake El'gygytgyn is a peculiar example of a continuous sedimentation history with $\delta^{18}O_{BSi}$ showing glacial–interglacial cycles at least back to MIS 9 (Chapligin et al., 2012b), which have been attributed by the authors to T_{air} changes. In addition to glacial–interglacial cycles, it is also possible to compare $\delta^{18}O_{BSi}$ of interglacials, i.e. MIS 1, MIS 5, MIS 11, when diatoms during cold stages are absent. In the sedimentary records of Lake El'gygytgyn, Chapligin (2012) investigated the $\delta^{18}O_{BSi}$ differences between the warm stages MIS 1, MIS 5 and MIS 11 and found MIS 11 as warmest interglacial. This interpretation has been supported by pollen–based T_{air} reconstructions by Melles et al. (2012) and underlines the applicability of the $\delta^{18}O_{BSi}$ proxy on glacial–interglacial timescales. Studies on Lake Baikal have also investigated past interglacials and have addressed changes in precipitation intermittency and cooling events during MIS 11 (Mackay et al., 2008). During MIS 5, millennial–scale variability is suggested to have been more stable than during MIS 1 (Mackay et al., 2013).

https://doi.org/10.5194/cp-2022-96
Preprint. Discussion started: 24 January 2023


Climate of the Past Discussions

Older $\delta^{18}O_{BSi}$ records do exist and often rely on paleo–lakes i.e. Ribains Maar, Baringo–Bogoria Basin, Makgadikgadi and Dethlingen (Shemesh et al., 2001b; Koutsodendris et al., 2012; Wilson et al., 2014b; Schmidt et al., 2017). These offer the possibility of extending the picture past still existing lakes, however lacking (present) hydrological constraints, which makes their interpretation and comparison to other, better-constrained records more challenging. Further research on $\delta^{18}O_{BSi}$ is therefore needed in order to complement the picture and provide insight into past climate and environmental conditions in continental regions, particularly valuable for high latitude and high–altitude regions poorly covered by other proxy data. Hydrologically open lakes with a long, continuous sedimentation history are most promising for extending climate reconstructions further into the past.

5. Conclusions

In this study, we have identified and gathered the existing lacustrine $\delta^{18}O_{BSi}$ records published to date in order to generate an added value by unifying them into a first $\delta^{18}O_{BSi}$ data compilation. We have identified 53 $\delta^{18}O_{BSi}$ records derived from 71 publications. These records stem from the entire globe with their geographical distribution focusing on high altitude and high latitude lacustrine environments. Diatoms bear the advantage of being available in dilute, non–alkaline lakes common in these environments. Regional clusters of records (e.g. northern Eurasia, East Africa) indicative of the research foci of the individual research groups employing the $\delta^{18}O_{BSi}$ proxy allow for generating regional subsets of data. Temporal coverage stretches from sub–recent timescales to the Pliocene which highlights the applicability of $\delta^{18}O_{BSi}$ on different timescales. Best coverage is available in MIS 1 which is linked to the age of lakes, and hence the availability of lake sediments, especially in high latitudes. Moreover, biogenic silica (here entirely diatom–based) is most abundant during warm periods (interstadials and interglacials) compared to colder periods. The interpretability of $\delta^{18}O_{BSi}$ records relies on regional setting, hydrological constraints of individual lakes and catchments, and preferably supported by isotope measurements of present lake water. Most $\delta^{18}O_{BSi}$ records stem from open lakes (N= 41), suggesting for these lakes a negligible influence of lake evaporation. In contrast, closed lakes (N=12) and paleo–lakes (N=9) have been investigated less. It has to be noted that a lake's ontogeny and hydrology may change throughout time and thus, hydrological changes constitute an approach for interpreting these $\delta^{18}O_{BSi}$ records.

Spatial resolution of the $\delta^{18}O_{BSi}$ records is determined by the size of the lake and its corresponding catchment with lake water effectively integrating the input signal. While this regional signal may integrate large areas such as in the case of lake Baikal, most catchments (N=18) are <100 km^2, suggesting a locally confined signal for these lakes. Regarding temporal resolution, most records feature sampling resolutions which by far exceed t_{res}, suggesting sampling resolution to be the decisive factor in determining a record's signal. However, in case of t_{res} >100yrs, lakes may be subject to increased lake evaporation.

https://doi.org/10.5194/cp-2022-96
Preprint. Discussion started: 24 January 2023

Accounting for offsets and different temporal resolution of records and filtering for similar hydrological settings (hydrologically open lakes with t_{res}<100 yrs), we find a common pattern throughout the Common Era at the centennial scale, which we attribute to changing hydroclimate conditions. Changes are similar between Eurasia and North America, but they still differ in the timing of $\delta^{18}O_{BSi}$ maxima. Generally, the combined Eurasian $\delta^{18}O_{BSi}$ record seems to include major climate episodes during this period, including Roman Climate Optimum, Migration Period Pessimum, Medieval Climatic Anomaly (MCA) and Little Ice Age. An effect of recent warming is not visible in the Common Era data, likely due to a lack of records meeting the filter criteria.

For the entire Holocene (MIS 1) in Eurasia and the NH (for hydrologically open lakes with t_{res}<100 yrs), we find a common decreasing $\delta^{18}O_{BSi}$ trend on the millennial scale which roughly follows summer insolation. The timing of the absolute $\delta^{18}O_{BSi}$ maxima of individual records in Eurasia differs and shows an east–west gradient with eastern Eurasian records featuring earlier Holocene maxima compared to western Eurasian records. Holocene minima occur within the last 2000 kyrs for all Eurasian records. North American records diverge from this MIS 1 pattern with later maxima and earlier minima. This behaviour is likely linked to atmospheric circulation patterns as also described by the authors of the individual records.

Extending the millennial–scale trend of Eurasian records into MIS 2 shows generally lower $\delta^{18}O_{BSi}$ values in MIS 2, suggesting lower T_{air} (and not P/E) in Glacial times, also visible in most other records that act on glacial–interglacial timescales. The applicability of the $\delta^{18}O_{BSi}$ proxy beyond MIS 2 is generally constrained by the availability of lake sediments and the abundance of diatoms in the respective sediments. Lake El'gygytgyn, as a prime example of hydrological continuity, displays glacial–interglacial cycles in the $\delta^{18}O_{BSi}$ record, supporting T_{air} being a prominent driver of $\delta^{18}O_{BSi}$ on millennial time scales. In Glacial periods, diatoms abundances are low, and this limitation does sometimes not allow for oxygen isotope analysis. However, comparison between interglacials where diatoms are generally more abundant, is feasible, i.e. at Lake Baikal and Lake El'gygytgyn. In summary, we demonstrate the applicability and intercomparability of combined $\delta^{18}O_{BSi}$ records into a first lacustrine $\delta^{18}O_{BSi}$ compilation allow for paleoclimate reconstructions, when accounting for regional offsets, different temporal resolutions and hydrological backgrounds. $\delta^{18}O_{BSi}$ records compiled in this study are, thus, an important tool for reconstructing paleoclimate across the globe and across a variety of time scales. In NH extratropic regions, their T_{air}–driven, quantitative signal makes them especially usable for use in conjunction with paleoclimate models. Future research would be most valuable in complementing the existing data with longer records (covering MIS 2 and beyond) as well as records from regions underrepresented thus far (especially the southern hemisphere).

https://doi.org/10.5194/cp-2022-96
Preprint. Discussion started: 24 January 2023

Climate of the Past Discussions
Open Access
EGU

Appendices

Appendix A

Figure A1. Geographical distribution of published $\delta^{18}O_{BSi}$ records and year of publication (N=64).

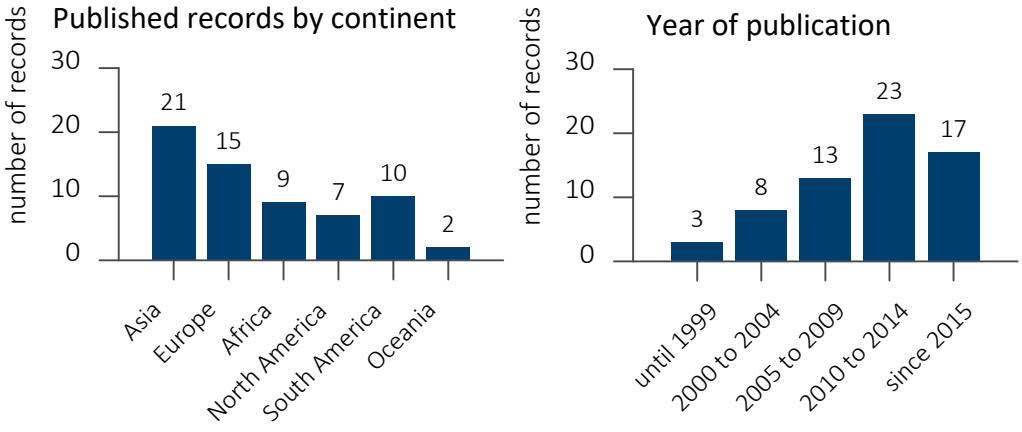

685

https://doi.org/10.5194/cp-2022-96
Preprint. Discussion started: 24 January 2023

Climate of the Past Discussions
Open Access
EGU

Figure A2. Overview of the dating methods used for age-model creation of published $\delta^{18}O_{BSi}$ time-series (N=64). Note that a single record can rely on multiple methods.

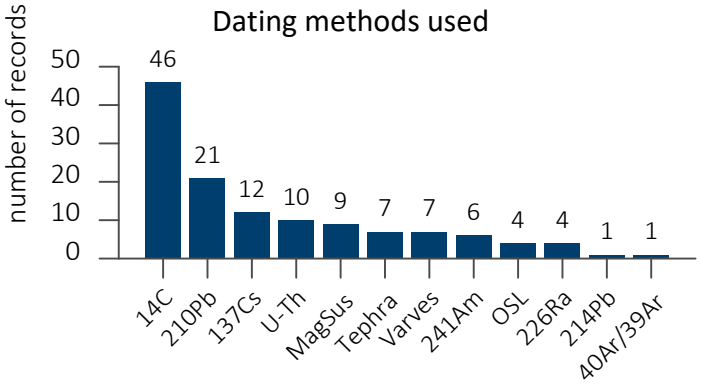

https://doi.org/10.5194/cp-2022-96
Preprint. Discussion started: 24 January 2023

Climate of the Past Discussions

690 **Figure A3. Overview of isotope hydrological background information considered in publications presenting $\delta^{18}O_{BSi}$ records (N=64).**

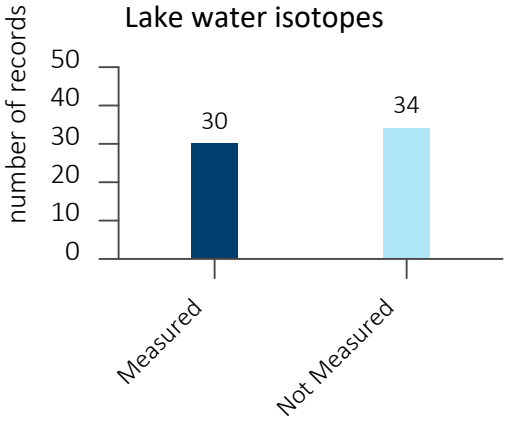

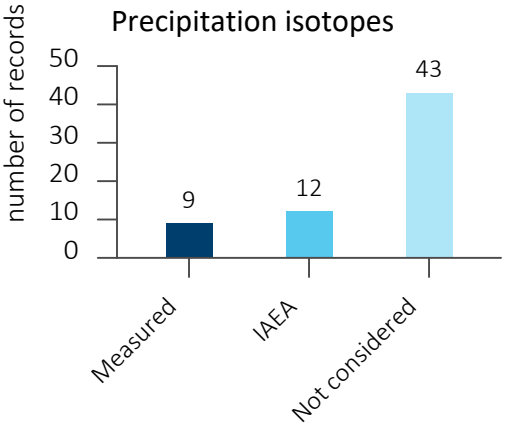

https://doi.org/10.5194/cp-2022-96
Preprint. Discussion started: 24 January 2023

Climate of the Past Discussions

Figure A4. Hydrological settings of the lakes corresponding to the $\delta^{18}O_{BSi}$ records compiled in this study, as indicated in the original publications (N=64). Owing to a lack of present constraints, paleo lakes are listed as a separate category.

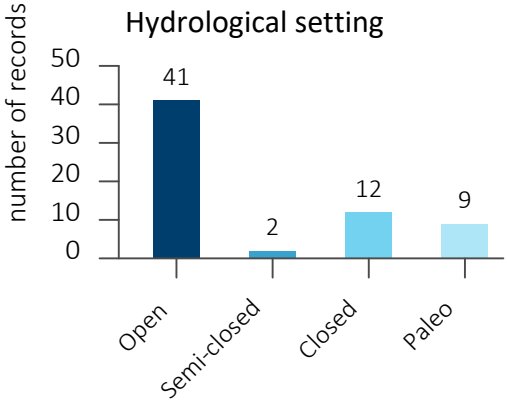

695

https://doi.org/10.5194/cp-2022-96
Preprint. Discussion started: 24 January 2023

Climate of the Past Discussions
Open Access
EGU

697 **Table A1. Overview of the records compiled and analyzed in this study. Lake basin parameters shown are taken from the HydroLakes database ((Messager et al., 2016) for consistency. In**
698 **case of major discrepancies between the HydroLakes database and the values provided by individual case studies, values of case studies are given in brackets and marked with an asterisk.**

699

700

No.	Archive	Lake	Short Reference	Lat. [dec deg]	Lon. [dec deg]	Water depth [m]	Altitude [m asl]	Lake Area [km2]	Catchment Area [km2]	Residence time [a]	Chron.	Rec_ID
1	Paleo Lake	Baringo-Bogoria Basin	Wilson et al. (2014b)	0.55	35.94		1178				Y	BD4
2	Lake	Baikal	Mackay et al. (2008)	53.70	108.35	321	449	31968	569176	375	Y	BDP962
3	Lake	El'gygytgyn	Chapligin et al. (2012b)	67.50	172.08	170	471	119	292	64	Y	Lz1024
4	Lake	Baikal	Mackay et al. (2013)	53.96	108.91	386	449	31968	569176	375	Y	CON016032
5	Paleo Lake	Ribains Maar	Shemesh et al. (2001b)	44.84	3.82		1074				N	RM1
6	Paleo Lake	Makgadikgadi	Schmidt et al. (2017)	-20.29	24.27		934				N	MBG1
7	Lake	Lake Pinarbasi	Leng et al. (2001)	37.47	33.12		1000	0.002			Y	PN94C
8	Lake	Kotokel Lake	Kostrova et al. (2013a); Kostrova et al. (2013b); Kostrova et al. (2014); Kostrova et al. (2016)	52.78	108.12	4	453	65.7	170	58	Y	KTK2
9	Lake	Baikal	Kalmychkov et al. (2007)	53.75	108.41	348	449	31968	569176	375	N	LB0301
10	Lake	Baikal	Kalmychkov et al. (2007)	53.39	107.53	233	449	31968	569176	375	N	LB0402
11	Lake	Lake Rutundu	Street-Perrott et al. (2008)	-0.03	37.45	11	3078	0.40			Y	R1
12	Paleo Lake	Les Echets	Ampel et al. (2009)	45.90	4.93		267				Y	EC1
13	Lake	Lake Challa	Barker et al. (2011)	-3.32	37.42	94	878	4.12	6.4	86	Y	LCHA1
14	Lake	Lake Malawi	Barker et al. (2007)	-9.98	34.23	363	476	29544	128727	219	Y	M982P
15	Lake	El'gygytgyn	Chapligin et al. (2012b)	67.66	172.14	177.0	471	119	292	64	Y	Lz1029
16	Lake	Bolshoye Shchuchye	(Meyer et al., 2022)	67.88	66.32	132.0	186	11.80	227	5	Y	Co1321
17	Paleo Lake	Tauca	Quesada et al. (2015)	-19.16	-68.20		3685				Y	PTAU1
18	Lake	Laguna Verda Baja	Polissar et al. (2006)	8.86	-70.87	5	4170				Y	LVB1
19	Lake	Tonsberg Lake	Rosqvist et al. (1999)	-54.17	-36.69		70	0.01			Y	TL1
20	Lake	Baikal	Mackay et al. (2011)	51.58	104.85	600.0	449	31968	569176	375	Y	CON016053
21	Lake	Small Hall Tarn	Barker (2001)	-0.15	37.35		4289				Y	SHT1

https://doi.org/10.5194/cp-2022-96
Preprint. Discussion started: 24 January 2023

Climate of the Past Discussions
Open Access
EGU

No.	Archive	Lake	Short Reference	Lat. [dec deg]	Lon. [dec deg]	Water depth [m]	Altitude [m asl]	Lake Area [km2]	Catchment Area [km2]	Residence time [a]	Chron.	Rec_ID
22	Lake	Lake Brazi	Magyari et al. (2013)	45.40	22.90	1.1	1740	0.004	0.10	0.5	Y	TDB1
23	Lake	Nar Gölü	Dean et al. (2018)	38.34	34.46	25.0	1369	0.52	3.5	15	Y	NAR0110
24	Lake	Lake Emanda	Kostrova et al. (2021)	65.28	135.75	14.6	654	33.10	118	26	Y	Co1412
25	Lake	Baunt Lake	Harding et al. (2020)	55.19	113.03	33	1052	112	10256	1.1	Y	BNT1418
26	Lake	Sunken Island Lake	Broadman et al. (2020b)	60.59	-150.89	7	84	0.44	28.3	0.18	Y	SILMC
27	Lake	Grandfather Lake	Hu and Shemesh (2003)	60.80	-158.52	20	142	0.35			Y	GL1
28	Lake	Lago Chungara	Hernandez et al. (2008); Hernandez et al. (2010); Hernandez et al. (2011); Hernandez et al. (2013)	-18.25	-69.17	40	4556	21.27	265	289 (15*)	Y	LG1
29	Lake	Lake Gosciaz	Rozanski et al. (2010)	52.58	19.35	25	63	0.38	20.6	0.51	Y	G702
30	Lake	Linsley Pond	Shemesh and Peteet (1998)	41.30	-72.75	9	8	0.93			Y	LP1
31	Lake	Lake Ladoga	Kostrova et al. (2019)	60.98	30.68	111		17444	279581	11	Y	Co1309
32	Lake	Laguna Verde Alta	Polissar et al. (2006)	8.85	-70.87	3	4215				Y	LVA1
33	Lake	Garba Guracha	Bittner et al. (2021)	6.88	39.88	5	3950	0.15	0.15		Y	BALGGU171
34	Lake	Simba Tarn	Barker (2001)	-0.15	37.32		4959	0.00			Y	ST1
35	Lake	Heart Lake	Bailey et al. (2018)	51.85	-176.69	7.6	60	0.25	8	0.038	Y	HL1
36	Lake	Mica Lake	Schiff et al. (2009)	60.96	-148.15	58	93	0.63	3.2	0.46	Y	MC2
37	Lake	Lake 850	Shemesh et al. (2001a)	68.25	19.12	8	850		0.5		Y	L850
38	Lake	Lake Chuna	Jones et al. (2004)	67.95	32.48		475	0.13	2	0.30	Y	LC1
39	Lake	Schrader Pond	Broadman et al. (2020a)	69.36	-145.08		869				Y	SCP162A
40	Lake	Lake Tilo	Lamb et al. (2005)	7.06	38.10	10	1551	0.66	144	0.15	Y	LT1
41	Lake	Nettilling Lake	Chapligin et al. (2016b); Narancic et al. (2016)	66.50	-70.50	14	18	4872.70	63400	5.5	N	Ni2B
42	Lake	Lake Pupuke	Heyng et al. (2015)	-36.78	174.77	58	11	1.01	1	5.8	Y	P210/P260
43	Lake	Vuolep Allakasjaure	Jonsson et al. (2010)	68.18	18.17	11	991	1.01	1	5.8	Y	VA
44	Lake	Lac Petit	Cartier et al. (2019a)	44.11	7.19	7	2200	0.018	6		Y	PET09P2
45	Lake	Two-Yurts Lake	Meyer et al. (2015a)	56.82	160.11	28	264	0.02	6		Y	PG1857
46	Lake	Hausberg Tarn	Rietti-Shati et al. (1998)	-0.15	37.30		4369	11.39	206	1.9	Y	

https://doi.org/10.5194/cp-2022-96
Preprint. Discussion started: 24 January 2023

Climate of the Past Discussions
Open Access
EGU

No.	Archive	Lake	Short Reference	Lat. [dec deg]	Lon. [dec deg]	Water depth [m]	Altitude [m asl]	Lake Area [km2]	Catchment Area [km2]	Residence time [a]	Chron.	Rec_ID
47	Lake	Laguna Zacapu	Leng et al. (2005)	19.83	-101.79	2.0	1987	0.23	66	0.037	N	ZAC3
48	Lake	Lake Stuor Goussasjavri	Rosqvist et al. (2013)	67.85	19.68	6	559	0.28	0.5	5.6	Y	LSG1
49	Lake	Lake Spaime	Rosqvist et al. (2013)	63.12	12.32	4	887	0.03	3.5	0.04	Y	LS1
50	Lake	Laguna Zacapu	Leng et al. (2005)	19.82	-101.79	8	1987	0.23	66	0.037	N	ZK2
51	Lake	Baikal	Swann et al. (2018)	51.77	104.42	1360	449	31968	569176	375	Y	BAIK13
52	Paleo Lake	Dethlingen	Koutsodendris et al. (2012)	52.96	10.14		65				N	D110
53	Lake	Yellowstone Lake	(Brown et al., 2021)	44.54	-110.39	61	2360	340	2579	21 (14*)	Y	YL16-2C

701

https://doi.org/10.5194/cp-2022-96
Preprint. Discussion started: 24 January 2023

Climate of the Past Discussions

Table A2. Overview of the records and corresponding publications identified by this study.

Rec_ID	*Archive*	*Lake*	*Core Type*	*original Core ID*	*Field Campaign (Year)*	*Short Reference*
EC1	Paleo Lake	Les Echets	single	EC1	2001	Ampel et al. (2009)
HL1	Lake	Heart Lake	Composite	10-AS-1D; 09-AS-1A; 09-AS-1B	2009, 2010	Bailey et al. (2018)
LCHA1	Lake	Lake Challa	composite	03-2K; 05-4P	2003	Barker et al. (2011)
M982P	Lake	Lake Malawi	single	M98-2P	1998	Barker et al. (2007)
SHT1	Lake	Small Hall Tarn			1996	Barker et al. (2001)
ST1	Lake	Simba Tarn			1996	Barker et al. (2001)
BALGGU171	Lake	Garba Guracha	composite	BAL-GGU17-1A; BAL-GGU17-1B	2017	Bittner et al. (2021)
SCP162A	Lake	Schrader Pond	single	SCP16-2A	2016	Broadman et al. (2020a)
SILMC	Lake	Sunken Island Lake	composite	SIL-MC	2017	Broadman et al. (2020b)
YL16-2C	Lake	Yellowstone Lake	composite	YL16-2C-1K; YL17-13A-1G	2016	Brown et al. (2021)
PET09P2	Lake	Lac Petit	single	PET09P2	2009	Cartier et al. (2019b)
Ni2B	Lake	Nettilling Lake	supplemented	Ni-2B	2012	Chapligin et al. (2016a)
Lz1024	Lake	El'gygytgyn	single	Lz1024	2003	Chapligin et al. (2012b)
LALB94	Lake	Lake Albano	supplemented	6A, 6B	1994	Chondrogianni et al. (2004)
NAR0110	Lake	Nar Gölü	single	NAR01/02	2001	Dean et al. (2018)
NAR0110	Lake	Nar Gölü	single	NAR10	2010	Dean et al. (2018)
BNT1418	Lake	Baunt Lake	Composite	BNT14	2014	Harding et al. (2020)
LG1	Lake	Lago Chungara	composite	10; 11	2002	Hernandez et al. (2011)
LCHUN02	Lake	Lago Chungara	composite	10; 11	2002	Hernandez et al. (2008)
LG1	Lake	Lago Chungara	composite	10; 11	2002	Hernandez et al. (2013)
LCHUN02	Lake	Lago Chungara	composite	10; 11	2002	Hernandez et al. (2010)
P2	Lake	Lake Pupuke	single	P2	2001	Heyng et al. (2015)
GL1	Lake	Grandfather Lake	single			Hu and Shemesh (2003)
ARL1	Lake	Arolik Lake				Hu et al. (2003)
LCHUN96	Lake	Lake Chuna	composite		1996	Jones et al. (2004)
SS1	Lake	Lake Spaime	single	SS1	2002	Jonsson et al. (2010)
VA	Lake	Vuolep Allakasjaure	supplemented	VAY1	2006	Jonsson et al. (2010)
LB0301	Lake	Lake Baikal	single	03-01		Kalmychkov et al. (2007)
LB0402	Lake	Lake Baikal	single	04-02		Kalmychkov et al. (2007)
Co1412	Lake	Lake Emanda	single	Co 1412	2017	Kostrova et al. (2021)
Co1309	Lake	Lake Ladoga	single	Co 1309	2013	Kostrova et al. (2019)
KTK2	Lake	Kotokel Lake	single	KTK2	2005	Kostrova et al. (2013a)
KTK2	Lake	Kotokel Lake	single	KTK2	2005	Kostrova et al. (2013b)
KTK2	Lake	Kotokel Lake	single	KTK2	2005	Kostrova et al. (2014)
KTK2	Lake	Kotokel Lake	single	KTK2	2005	Kostrova et al. (2016)

https://doi.org/10.5194/cp-2022-96
Preprint. Discussion started: 24 January 2023


Climate of the Past Discussions

Rec_ID	*Archive*	*Lake*	*Core Type*	*original Core ID*	*Field Campaign (Year)*	*Short Reference*
D1	Paleo Lake	Dethlingen	single		2004	Koutsodendris et al. (2012)
LT1	Lake	Lake Tilo	composite	T97; T95	1995	Lamb et al. (2005)
PN94C	Lake	Lake Pinarbasi	single	PN94C	1994	Leng et al. (2001)
ZAC3	Lake	Laguna Zacapu	single	ZAC/3	2001	Leng et al. (2005)
ZK2	Lake	Laguna Zacapu	single	ZK2	2001	Leng et al. (2005)
BDP962	Lake	Lake Baikal	single	BDP-96-2	1996	Mackay et al. (2008)
CON016053	Lake	Lake Baikal	supplemented	CON01-605-3	2001	Mackay et al. (2011)
CON016032	Lake	Lake Baikal	single	CON-01-603-2	2001	Mackay et al. (2013)
TDB1	Lake	Lake Brazi	single	TDB-1	2007	Magyari et al. (2013)
Co1321	Lake	Bolshoye Shchuchye	single	Co1321	2016	(Meyer et al., 2022)
PG1857	Lake	Two-Yurts Lake	composite	PG1857; PG1857-2	2007	Meyer et al. (2015a)
CON016053	Lake	Lake Baikal	supplemented	CON01-605-3	2001	Morley et al. (2005)
LVA1	Lake	Laguna Verde Alta	composite			Polissar et al. (2006)
LVB1	Lake	Laguna Verda Baja	supplemented			Polissar et al. (2006)
PTAU1	Paleo Lake	Tauca	supplemented	BT		Quesada et al. (2015)
PTAU1	Paleo Lake	Tauca	supplemented	CB		Quesada et al. (2015)
PTAU1	Paleo Lake	Tauca	supplemented	EWK		Quesada et al. (2015)
PTAU1	Paleo Lake	Tauca	supplemented	PJ		Quesada et al. (2015)
HT1	Lake	Hausberg Tarn			1996	Rietti-Shati et al. (1998)
VA	Lake	Vuolep Allakasjaure	supplemented	VA2	2000	Rosqvist et al. (2004)
LS1	Lake	Lake Spaime	supplemented	Core III	2006	Rosqvist et al. (2013)
LSG1	Lake	Lake Stuor Goussasjavri	supplemented	Core III	2007	Rosqvist et al. (2013)
TL1	Lake	Tonsberg Lake	composite		1991	Rosqvist et al. (1999)
G702	Lake	Lake Gosciaz	supplemented	G7/02	2002	Rozanski et al. (2010)
MC2	Lake	Mica Lake	supplemented	MC-2	2006	Schiff et al. (2009)
MBG1	Paleo Lake	Makgadikgadi	outcrop		2011	Schmidt et al. (2017)
RM1	Paleo Lake	Ribains Maar	single		1988	Shemesh et al. (2001b)
LP1	Lake	Linsley Pond	supplemented		1987	Shemesh and Peteet (1998)
L850	Lake	Lake 850	single		1999	Shemesh et al. (2001a)
R1	Lake	Lake Rutundu	single	R-1	1996	Street-Perrott et al. (2008)
BAIK13	Lake	Lake Baikal	single	BAIK13-1	2013	Swann et al. (2018)
BAIK13	Lake	Lake Baikal	single	BAIK13-4	2013	Swann et al. (2018)
BAIK13	Lake	Lake Baikal	single	BAIK13-5	2013	Swann et al. (2018)
BAIK13	Lake	Lake Baikal	single	BAIK13-7	2013	Swann et al. (2018)

https://doi.org/10.5194/cp-2022-96
Preprint. Discussion started: 24 January 2023

Data availability

The dataset is being submitted to PANGAEA.

Author contributions

PM, HM, BD and BB designed the research project and structure of the manuscript. PM compiled the data base, carried out statistical analyses and produced all figures and tables and wrote the main part of the manuscript. ML, GR, EB, AH, GS, AM, HM, HB and PB contributed data publicly not available. All co-authors brought in their expertise have made substantial contributions to the manuscript. All authors have written parts of the manuscript, commented on drafts and have approved its final submitted version.

Competing Interests

The authors declare that they have no conflict of interest.

Disclaimer

Maps throughout this article were created using ArcGIS® software by Esri. ArcGIS® and ArcMap™ are the intellectual property of Esri and are used herein under license. Copyright © Esri. All rights reserved. For more information about Esri® software, please visit www.esri.com.'

Acknowledgements

PM is funded by German Ministry of Education and Research via the Palmod2-Projek (01LP1923B). HB is funded by the Academy of Finland (grant 348536). AH is funded by the Spanish Ministry of Science and Innovation through the Ramón y Cajal Scheme (RYC2020-029253-I). We thank xx (anonymous) reviewers whose comments helped improving the manuscript. We also thank all scientists and technicians developing and advancing the research field of oxygen isotopes in diatom silica.

https://doi.org/10.5194/cp-2022-96
Preprint. Discussion started: 24 January 2023

References

Ampel, L., Wohlfarth, B., Risberg, J., Veres, D., Leng, M. J., and Tillman, P. K.: Diatom assemblage dynamics during abrupt climate change: the response of lacustrine diatoms to Dansgaard–Oeschger cycles during the last glacial period, J Paleolimnol, 44, 397-404, 10.1007/s10933-009-9350-7, 2009.

Andersen, K. K., Azuma, N., Barnola, J. M., Bigler, M., Biscaye, P., Caillon, N., Chappellaz, J., Clausen, H. B., Dahl-Jensen, D., Fischer, H., Flückiger, J., Fritzsche, D., Fujii, Y., Goto-Azuma, K., Grønvold, K., Gundestrup, N. S., Hansson, M., Huber, C., Hvidberg, C. S., Johnsen, S. J., Jonsell, U., Jouzel, J., Kipfstuhl, S., Landais, A., Leuenberger, M., Lorrain, R., Masson-Delmotte, V., Miller, H., Motoyama, H., Narita, H., Popp, T., Rasmussen, S. O., Raynaud, D., Rothlisberger, R., Ruth, U., Samyn, D., Schwander, J., Shoji, H., Siggard-Andersen, M. L., Steffensen, J. P., Stocker, T., Sveinbjörnsdóttir, A. E., Svensson, A., Takata, M., Tison, J. L., Thorsteinsson, T., Watanabe, O., Wilhelms, F., White, J. W. C., and North Greenland Ice Core Project, m.: High-resolution record of Northern Hemisphere climate extending into the last interglacial period, Nature, 431, 147-151, 10.1038/nature02805, 2004.

Bailey, H. L., Kaufman, D. S., Sloane, H. J., Hubbard, A. L., Henderson, A. C. G., Leng, M. J., Meyer, H., and Welker, J. M.: Holocene atmospheric circulation in the central North Pacific: A new terrestrial diatom and δ18O dataset from the Aleutian Islands, Quaternary Sci Rev, 194, 27-38, 10.1016/j.quascirev.2018.06.027, 2018.

Barker, P. A.: A 14,000-Year Oxygen Isotope Record from Diatom Silica in Two Alpine Lakes on Mt. Kenya, Science, 292, 2307-2310, 10.1126/science.1059612, 2001.

Barker, P. A., Leng, M. J., Gasse, F., and Huang, Y.: Century-to-millennial scale climatic variability in Lake Malawi revealed by isotope records, Earth Planet Sc Lett, 261, 93-103, 10.1016/j.epsl.2007.06.010, 2007.

Barker, P. A., Hurrell, E. R., Leng, M. J., Wolff, C., Cocquyt, C., Sloane, H. J., and Verschuren, D.: Seasonality in equatorial climate over the past 25 k.y. revealed by oxygen isotope records from Mount Kilimanjaro, Geology, 39, 1111-1114, 10.1130/g32419.1, 2011.

Barker, P. A., Street-Perrott, F. A., Leng, M. J., Greenwood, P. B., Swain, D. L., Perrott, R. A., Telford, R. J., and Ficken, K. J.: A 14,000-year oxygen isotope record from diatom silica in two alpine lakes on Mt. Kenya, Science, 292, 2307-2310, DOI 10.1126/science.1059612, 2001.

Biskaborn, B. K., Subetto, D. A., Savelieva, L. A., Vakhrameeva, P. S., Hansche, A., Herzschuh, U., Klemm, J., Heinecke, L., Pestryakova, L. A., Meyer, H., Kuhn, G., and Diekmann, B.: Late Quaternary vegetation and lake system dynamics in north-eastern Siberia: Implications for seasonal climate variability, Quaternary Sci Rev, 147, 406-421, https://doi.org/10.1016/j.quascirev.2015.08.014, 2016.

Bittner, L., Gil-Romera, G., Grady, D., Lamb, H. F., Lorenz, E., Weiner, M., Meyer, H., Bromm, T., Glaser, B., and Zech, M.: The Holocene lake-evaporation history of the afro-alpine Lake Garba Guracha in the Bale Mountains, Ethiopia, based on δ18O records of sugar biomarker and diatoms, Quaternary Res, 1-14, 10.1017/qua.2021.26, 2021.

The Online Isotopes in Precipitation Calculator version OIPC3.1: http://www.waterisotopes.org, last access: 8/2022.

Bradley, R. S., Hughes, M. K., and Diaz, H. F.: Climate in Medieval Time, Science, 302, 404-405, doi:10.1126/science.1090372, 2003.

Brewer, T. S., Leng, M. J., Mackay, A. W., Lamb, A. L., Tyler, J. J., and Marsh, N. G.: Unravelling contamination signals in biogenic silica oxygen isotope composition: the role of major and trace element geochemistry, J Quaternary Sci, 23, 321-330, https://doi.org/10.1002/jqs.1171, 2008.

Broadman, E., Kaufman, D. S., Henderson, A. C. G., Malmierca-Vallet, I., Leng, M. J., and Lacey, J. H.: Coupled impacts of sea ice variability and North Pacific atmospheric circulation on Holocene hydroclimate in Arctic Alaska, Proceedings of the National Academy of Sciences, 117, 33034-33042, 10.1073/pnas.2016544117, 2020a.

Broadman, E., Kaufman, D. S., Henderson, A. C. G., Berg, E. E., Anderson, R. S., Leng, M. J., Stahnke, S. A., and Muñoz, S. E.: Multi-proxy evidence for millennial-scale changes in North Pacific Holocene hydroclimate from the Kenai Peninsula lowlands, south-central Alaska, Quaternary Sci Rev, 241, 10.1016/j.quascirev.2020.106420, 2020b.

Brown, S. R., Cartier, R., Schiller, C. M., Zahajská, P., Fritz, S. C., Morgan, L. A., Whitlock, C., Conley, D. J., Lacey, J. H., Leng, M. J., and Shanks, W. C. P.: Multi-proxy record of Holocene paleoenvironmental conditions from Yellowstone Lake, Wyoming, USA, Quaternary Sci Rev, 274, 107275, https://doi.org/10.1016/j.quascirev.2021.107275, 2021.

Büntgen, U., Myglan, V. S., Ljungqvist, F. C., McCormick, M., Di Cosmo, N., Sigl, M., Jungclaus, J., Wagner, S., Krusic, P. J., Esper, J., Kaplan, J. O., de Vaan, M. A. C., Luterbacher, J., Wacker, L., Tegel, W., and Kirdyanov, A. V.: Cooling and societal change during the Late Antique Little Ice Age from 536 to around 660 AD, Nature Geoscience, 9, 231-236, 10.1038/ngeo2652, 2016.

Cartier, R., Sylvestre, F., Paillès, C., Sonzogni, C., Couapel, M., Alexandre, A., Mazur, J.-C., Brisset, E., Miramont, C., and Guiter, F.: Diatom-oxygen isotope record from high-altitude Lake Petit (2200 m a.s.l.) in the Mediterranean Alps: shedding light on a climatic pulse at 4.2 ka, Clim Past, 15, 253-263, 10.5194/cp-15-253-2019, 2019a.

Cartier, R., Sylvestre, F., Pailles, C., Sonzogni, C., Couapel, M., Alexandre, A., Mazur, J. C., Brisset, E., Miramont, C., and Guiter, F.: Diatom-oxygen isotope record from high-altitude Lake Petit (2200 m a.s.l.) in the Mediterranean Alps: shedding light on a climatic pulse at 4.2 ka, Clim Past, 15, 253-263, 10.5194/cp-15-253-2019, 2019b.

Chapligin, B., Narancic, B., Meyer, H., and Pienitz, R.: Paleo-environmental gateways in the eastern Canadian arctic – Recent isotope hydrology and diatom oxygen isotopes from Nettilling Lake, Baffin Island, Canada, Quaternary Sci Rev, 147, 379-390, 10.1016/j.quascirev.2016.03.028, 2016a.

https://doi.org/10.5194/cp-2022-96
Preprint. Discussion started: 24 January 2023

Chapligin, B., Narancic, B., Meyer, H., and Pienitz, R.: Paleo-environmental gateways in the eastern Canadian arctic - Recent isotope hydrology and diatom oxygen isotopes from Nettilling Lake, Baffin Island, Canada, Quaternary Sci Rev, 147, 379-390, 10.1016/j.quascirev.2016.03.028, 2016b.

Chapligin, B., Meyer, H., Bryan, A., Snyder, J., and Kemnitz, H.: Assessment of purification and contamination correction methods for analysing the oxygen isotope composition from biogenic silica, Chem Geol, 300, 185-199, 10.1016/j.chemgeo.2012.01.004, 2012a.

Chapligin, B., Meyer, H., Swann, G. E. A., Meyer-Jacob, C., and Hubberten, H. W.: A 250 ka oxygen isotope record from diatoms at Lake El'gygytgyn, far east Russian Arctic, Clim Past, 8, 1621-1636, 10.5194/cp-8-1621-2012, 2012b.

Chapligin, B., Leng, M. J., Webb, E., Alexandre, A., Dodd, J. P., Ijiri, A., Lücke, A., Shemesh, A., Abelmann, A., Herzschuh, U., Longstaffe, F. J., Meyer, H., Moschen, R., Okazaki, Y., Rees, N. H., Sharp, Z. D., Sloane, H. J., Sonzogni, C., Swann, G. E. A., Sylvestre, F., Tyler, J. J., and Yam, R.: Inter-laboratory comparison of oxygen isotope compositions from biogenic silica, Geochim Cosmochim Ac, 75, 7242-7256, https://doi.org/10.1016/j.gca.2011.08.011, 2011.

Chapligin, B., Meyer, Hanno , Langer, Moritz and Hubberten, Hans-Wolfgang: A 250 ka oxygen isotope record from diatoms and investigation of "super-interglacial" conditions during MIS 11 at Lake El'gygytgyn, Far East Russian Arctic. , AGU Fall Meeting 2012, San Francisco, USA, 3 December 2012 - 7 December 2012 . ,

Chondrogianni, C., Ariztegui, D., Rolph, T., Juggins, S., Shemesh, A., Rietti-Shati, M., Niessen, F., Guilizzoni, P., Lami, A., McKenzie, J. A., and Oldfield, F.: Millennial to interannual climate variability in the Mediterranean during the Last Glacial Maximum, Quatern Int, 122, 31-41, 10.1016/j.quaint.2004.01.029, 2004.

DANEK, C., GIERZ, P., KOSTROVA, S. S., MEISTER, P., MEYER, H., and WERNER, M.: Eurasian Holocene climate trends in transient coupled climate simulations and stable oxygen isotope records, J Quaternary Sci, n/a, https://doi.org/10.1002/jqs.3396, 2021.

Dansgaard, W.: Stable isotopes in precipitation, Tellus, 16, 436-468, https://doi.org/10.1111/j.2153-3490.1964.tb00181.x, 1964.

Dean, J. R., Jones, M. D., Leng, M. J., Metcalfe, S. E., Sloane, H. J., Eastwood, W. J., and Roberts, C. N.: Seasonality of Holocene hydroclimate in the Eastern Mediterranean reconstructed using the oxygen isotope composition of carbonates and diatoms from Lake Nar, central Turkey, Holocene, 28, 267-276, 10.1177/0959683617721326, 2018.

Dodd, J. P. and Sharp, Z. D.: A laser fluorination method for oxygen isotope analysis of biogenic silica and a new oxygen isotope calibration of modern diatoms in freshwater environments, Geochim Cosmochim Ac, 74, 1381-1390, 10.1016/j.gca.2009.11.023, 2010.

Harding, P., Bezrukova, E. V., Kostrova, S. S., Lacey, J. H., Leng, M. J., Meyer, H., Pavlova, L. A., Shchetnikov, A., Shtenberg, M. V., Tarasov, P. E., and Mackay, A. W.: Hydrological (in)stability in Southern Siberia during the Younger Dryas and early Holocene, Global Planet Change, 195, 10.1016/j.gloplacha.2020.103333, 2020.

Helama, S., Jones, P. D., and Briffa, K. R.: Dark Ages Cold Period: A literature review and directions for future research, The Holocene, 27, 1600-1606, 10.1177/0959683617693898, 2017.

Hernandez, A., Giralt, S., Bao, R., Saez, A., Leng, M. J., and Barker, P. A.: ENSO and solar activity signals from oxygen isotopes in diatom silica during late glacial-Holocene transition in Central Andes (18A degrees S), J Paleolimnol, 44, 413-429, 10.1007/s10933-010-9412-x, 2010.

Hernandez, A., Bao, R., Giralt, S., Barker, P. A., Leng, M. J., Sloane, H. J., and Saez, A.: Biogeochemical processes controlling oxygen and carbon isotopes of diatom silica in Late Glacial to Holocene lacustrine rhythmites, Palaeogeogr Palaeocl, 299, 413-425, 10.1016/j.palaeo.2010.11.020, 2011.

Hernandez, A., Bao, R., Giralt, S., Saez, A., Leng, M. J., Barker, P. A., Kendrick, C. P., and Sloane, H. J.: Climate, catchment runoff and limnological drivers of carbon and oxygen isotope composition of diatom frustules from the central Andean Altiplano during the Lateglacial and Early Holocene, Quaternary Sci Rev, 66, 64-73, 10.1016/j.quascirev.2012.10.013, 2013.

Hernandez, A., Bao, R., Giralt, S., Leng, M. J., Barker, P. A., Saez, A., Pueyo, J. J., Moreno, A., Valero-Garces, B. L., and Sloane, H. J.: The palaeohydrological evolution of Lago Chungara (Andean Altiplano, northern Chile) during the Lateglacial and early Holocene using oxygen isotopes in diatom silica, J Quaternary Sci, 23, 351-363, 10.1002/jqs.1173, 2008.

Herzschuh, U., Birks, H. J. B., Laepple, T., Andreev, A., Melles, M., and Brigham-Grette, J.: Glacial legacies on interglacial vegetation at the Pliocene-Pleistocene transition in NE Asia, Nature Communications, 7, 11967, 10.1038/ncomms11967, 2016.

Herzschuh, U. B., Thomas; Li, Chenzhi; Cao, Xianyong: Northern Hemisphere temperature and precipitation reconstruction from taxonomically harmonized pollen data set with revised chronologies using WA-PLS and MAT (LegacyClimate 1.0). PANGAEA [dataset], https://doi.pangaea.de/10.1594/PANGAEA.930512, 2021.

Heyng, A. M., Mayr, C., Lücke, A., Moschen, R., Wissel, H., Striewski, B., and Bauersachs, T.: Middle and Late Holocene paleotemperatures reconstructed from oxygen isotopes and GDGTs of sediments from Lake Pupuke, New Zealand, Quatern Int, 374, 3-14, 10.1016/j.quaint.2014.12.040, 2015.

Hu, F. S. and Shemesh, A.: A biogenic-silica δ18O record of climatic change during the last glacial–interglacial transition in southwestern Alaska, Quaternary Res, 59, 379-385, 10.1016/s0033-5894(03)00056-5, 2003.

Hu, F. S., Kaufman, D., Yoneji, S., Nelson, D., Shemesh, A., Huang, Y., Tian, J., Bond, G., Clegg, B., and Brown, T.: Cyclic Variation and Solar Forcing of Holocene Climate in the Alaskan Subarctic, Science, 301, 1890-1893, doi:10.1126/science.1088568, 2003.

IAEA/WMO: Global Network of Isotopes in Precipitation. The GNIP Database. [dataset], 2022.

https://doi.org/10.5194/cp-2022-96
Preprint. Discussion started: 24 January 2023

Jones, V. J., Leng, M. J., Solovieva, N., Sloane, H. J., and Tarasov, P.: Holocene climate of the Kola Peninsula; evidence from the oxygen isotope record of diatom silica, Quaternary Sci Rev, 23, 833-839, 10.1016/j.quascirev.2003.06.014, 2004.

Jonsson, C. E., Rosqvist, G. C., Leng, M. J., Bigler, C., Bergman, J., Tillman, P. K., and Sloane, H. J.: High-resolution diatom δ18O records, from the last 150 years, reflecting changes in amount of winter precipitation in two sub-Arctic high-altitude lakes in the Swedish Scandes, J Quaternary Sci, 25, 918-930, https://doi.org/10.1002/jqs.1372, 2010.

Kalmychkov, G., Kuz'min, M., Pokrovskii or Pokrovsky, B., and Kostrova, S.: Oxygen isotopic composition in diatom algae frustules from Lake Baikal sediments: Annual mean temperature variations during the last 40 Ka, Dokl Earth Sci, 413, 206-209, 10.1134/S1028334X07020158, 2007.

Kaufman, D., McKay, N., Routson, C., Erb, M., Dätwyler, C., Sommer, P. S., Heiri, O., and Davis, B.: Holocene global mean surface temperature, a multi-method reconstruction approach, Scientific Data, 7, 201, 10.1038/s41597-020-0530-7, 2020.

Kaufman, D. S., Ager, T. A., Anderson, N. J., Anderson, P. M., Andrews, J. T., Bartlein, P. J., Brubaker, L. B., Coats, L. L., Cwynar, L. C., Duvall, M. L., Dyke, A. S., Edwards, M. E., Eisner, W. R., Gajewski, K., Geirsdóttir, A., Hu, F. S., Jennings, A. E., Kaplan, M. R., Kerwin, M. W., Lozhkin, A. V., MacDonald, G. M., Miller, G. H., Mock, C. J., Oswald, W. W., Otto-Bliesner, B. L., Porinchu, D. F., Rühland, K., Smol, J. P., Steig, E. J., and Wolfe, B. B.: Holocene thermal maximum in the western Arctic (0–180°W), Quaternary Sci Rev, 23, 529-560, https://doi.org/10.1016/j.quascirev.2003.09.007, 2004.

Konecky, B. L., McKay, N. P., Churakova, O. V., Comas-Bru, L., Dassié, E. P., DeLong, K. L., Falster, G. M., Fischer, M. J., Jones, M. D., Jonkers, L., Kaufman, D. S., Leduc, G., Managave, S. R., Martrat, B., Opel, T., Orsi, A. J., Partin, J. W., Sayani, H. R., Thomas, E. K., Thompson, D. M., Tyler, J. J., Abram, N. J., Atwood, A. R., Cartapanis, O., Conroy, J. L., Curran, M. A., Dee, S. G., Deininger, M., Divine, D. V., Kern, Z., Porter, T. J., Stevenson, S. L., von Gunten, L., and Iso2k Project, M.: The Iso2k database: a global compilation of paleo-δ18O and δ2H records to aid understanding of Common Era climate, Earth Syst. Sci. Data, 12, 2261-2288, 10.5194/essd-12-2261-2020, 2020.

Kostrova, S. S., Meyer, H., Chapligin, B., Tarasov, P. E., and Bezrukova, E. V.: The last glacial maximum and late glacial environmental and climate dynamics in the Baikal region inferred from an oxygen isotope record of lacustrine diatom silica, Quatern Int, 348, 25-36, 10.1016/j.quaint.2014.07.034, 2014.

Kostrova, S. S., Biskaborn, B. K., Pestryakova, L. A., Fernandoy, F., Lenz, M. M., and Meyer, H.: Climate and environmental changes of the Lateglacial transition and Holocene in northeastern Siberia: Evidence from diatom oxygen isotopes and assemblage composition at Lake Emanda, Quaternary Sci Rev, 259, 106905, https://doi.org/10.1016/j.quascirev.2021.106905, 2021.

Kostrova, S. S., Meyer, H., Chapligin, B., Bezrukova, E. V., Tarasov, P. E., and Kuz'min, M. I.: Reconstruction of the Holocene climate of Transbaikalia: Evidence from the oxygen isotope analysis of fossil diatoms from Kotokel Lake, Dokl Earth Sci, 451, 732-736, 10.1134/S1028334x13070039, 2013a.

Kostrova, S. S., Meyer, H., Chapligin, B., Kossler, A., Bezrukova, E. V., and Tarasov, P. E.: Holocene oxygen isotope record of diatoms from Lake Kotokel (southern Siberia, Russia) and its palaeoclimatic implications, Quatern Int, 290, 21-34, 10.1016/j.quaint.2012.05.011, 2013b.

Kostrova, S. S., Meyer, H., Tarasov, P. E., Bezrukova, E. V., Chapligin, B., Kossler, A., Pavlova, L. A., and Kuzmin, M. I.: Oxygen isotope composition of diatoms from sediments of Lake Kotokel (Buryatia), Russ Geol Geophys+, 57, 1239-1247, 10.1016/j.rgg.2016.08.009, 2016.

Kostrova, S. S., Meyer, H., Bailey, H. L., Ludikova, A. V., Gromig, R., Kuhn, G., Shibaev, Y. A., Kozachek, A. V., Ekaykin, A. A., and Chapligin, B.: Holocene hydrological variability of Lake Ladoga, northwest Russia, as inferred from diatom oxygen isotopes, Boreas, 48, 361-376, 10.1111/bor.12385, 2019.

Koutsodendris, A., Pross, J., Müller, U. C., Brauer, A., Fletcher, W. J., Kühl, N., Kirilova, E., Verhagen, F. T. M., Lücke, A., and Lotter, A. F.: A short-term climate oscillation during the Holsteinian interglacial (MIS 11c): An analogy to the 8.2ka climatic event?, Global Planet Change, 92-93, 224-235, 10.1016/j.gloplacha.2012.05.011, 2012.

Kwiecien, O., Stockhecke, M., Pickarski, N., Heumann, G., Litt, T., Sturm, M., Anselmetti, F., Kipfer, R., and Haug, G. H.: Dynamics of the last four glacial terminations recorded in Lake Van, Turkey, Quaternary Sci Rev, 104, 42-52, https://doi.org/10.1016/j.quascirev.2014.07.001, 2014.

Lamb, A. L., Leng, M. J., Sloane, H. J., and Telford, R. J.: A comparison of the palaeoclimate signals from diatom oxygen isotope ratios and carbonate oxygen isotope ratios from a low latitude crater lake, Palaeogeogr Palaeocl, 223, 290-302, 10.1016/j.palaeo.2005.04.011, 2005.

Lasher, G., Axford, Y., McFarlin, J., Kelly, M., Osterberg, E., and Berkelhammer, M.: Holocene temperatures and isotopes of precipitation in Northwest Greenland recorded in lacustrine organic materials, Quaternary Sci Rev, 170, 45-55, 10.1016/j.quascirev.2017.06.016, 2017.

Laskar, J., Robutel, P., Joutel, F., Gastineau, M., Correia, A. C. M., and Levrard, B.: A long-term numerical solution for the insolation quantities of the Earth, A&A, 428, 261-285, 2004.

Leclerc, A. J. and Labeyrie, L.: Temperature dependence of the oxygen isotopic fractionation between diatom silica and water, Earth Planet Sc Lett, 84, 69-74, https://doi.org/10.1016/0012-821X(87)90177-4, 1987.

Leng, M., Barker, P., Greenwood, P., Roberts, N., and Reed, J.: Oxygen isotope analysis of diatom silica and authigenic calcite from Lake Pinarbasi, Turkey, J Paleolimnol, 25, 343-349, Doi 10.1023/A:1011169832093, 2001.

Leng, M. J.: Isotopes in palaeoenvironmental research, Developments in paleoenvironmental research :, 10, Springer, Dordrecht, xviii, 307 p. pp.2006.
Leng, M. J. and Barker, P. A.: A review of the oxygen isotope composition of lacustrine diatom silica for palaeoclimate reconstruction, Earth-Sci Rev, 75, 5-27, 10.1016/j.earscirev.2005.10.001, 2006.
Leng, M. J. and Marshall, J. D.: Palaeoclimate interpretation of stable isotope data from lake sediment archives, Quaternary Sci Rev, 23, 811-831, https://doi.org/10.1016/j.quascirev.2003.06.012, 2004.
Leng, M. J., Metcalfe, S. E., and Davies, S. J.: Investigating late holocene climate variability in central mexico using carbon isotope ratios in organic materials and oxygen isotope ratios from diatom silica within lacustrine sediments, J Paleolimnol, 34, 413-431, 10.1007/s10933-005-6748-8, 2005.
Lisiecki, L. E. and Raymo, M. E.: A Pliocene-Pleistocene stack of 57 globally distributed benthic δ18O records, Paleoceanography, 20, n/a-n/a, 10.1029/2004pa001071, 2005.
Ljungqvist, F. C.: A new reconstruction of temperature variability in the extra-tropical northern hemisphere during the last two millennia, Geografiska Annaler: Series A, Physical Geography, 92, 339-351, 10.1111/j.1468-0459.2010.00399.x, 2010.
Mackay, A. W., Karabanov, E., Leng, M. J., Sloane, H. J., Morley, D. W., Panizzo, V. N., Khursevich, G., and Williams, D.: Reconstructing hydrological variability in Lake Baikal during MIS 11: an application of oxygen isotope analysis of diatom silica, J Quaternary Sci, 23, 365-374, 10.1002/jqs.1174, 2008.
Mackay, A. W., Swann, G. E. A., Brewer, T. S., Leng, M. J., Morley, D. W., Piotrowska, N., Rioual, P., and White, D.: A reassessment of late glacial - Holocene diatom oxygen isotope record from Lake Baikal using a geochemical mass-balance approach, J Quaternary Sci, 26, 627-634, 10.1002/jqs.1484, 2011.
Mackay, A. W., Swann, G. E. A., Fagel, N., Fietz, S., Leng, M. J., Morley, D., Rioual, P., and Tarasov, P.: Hydrological instability during the Last Interglacial in central Asia: a new diatom oxygen isotope record from Lake Baikal, Quaternary Sci Rev, 66, 45-54, 10.1016/j.quascirev.2012.09.025, 2013.
Magyari, E. K., Demeny, A., Buczko, K., Kern, Z., Vennemann, T., Forizs, I., Vincze, I., Braun, M., Kovacs, J. I., Udvardi, B., and Veres, D.: A 13,600-year diatom oxygen isotope record from the South Carpathians (Romania): Reflection of winter conditions and possible links with North Atlantic circulation changes, Quatern Int, 293, 136-149, 10.1016/j.quaint.2012.05.042, 2013.
Mann, M. E., Zhang, Z., Rutherford, S., Bradley, R. S., Hughes, M. K., Shindell, D., Ammann, C., Faluvegi, G., and Ni, F.: Global Signatures and Dynamical Origins of the Little Ice Age and Medieval Climate Anomaly, Science, 326, 1256-1260, doi:10.1126/science.1177303, 2009.
Marcott, S., Shakun, J., Clark, P., and Mix, A.: A Reconstruction of Regional and Global Temperature for the Past 11,300 Years, Science (New York, N.Y.), 339, 1198-1201, 10.1126/science.1228026, 2013.
Matheney, R. K. and Knauth, L. P.: Oxygen-isotope fractionation between marine biogenic silica and seawater, Geochim Cosmochim Ac, 53, 3207-3214, 10.1016/0016-7037(89)90101-4, 1989.
Matthews, J. A. and Briffa, K. R.: The 'Little Ice Age': Re-Evaluation of an Evolving Concept, Geografiska Annaler. Series A, Physical Geography, 87, 17-36, 2005.
Melles, M., Brigham-Grette, J., Minyuk, P. S., Nowaczyk, N. R., Wennrich, V., DeConto, R. M., Anderson, P. M., Andreev, A. A., Coletti, A., Cook, T. L., Haltia-Hovi, E., Kukkonen, M., Lozhkin, A. V., Rosén, P., Tarasov, P., Vogel, H., and Wagner, B.: 2.8 Million Years of Arctic Climate Change from Lake El’gygytgyn, NE Russia, Science, 337, 315-320, doi:10.1126/science.1222135, 2012.
Messager, M. L., Lehner, B., Grill, G., Nedeva, I., and Schmitt, O.: Estimating the volume and age of water stored in global lakes using a geo-statistical approach, Nature Communications, 7, 13603, 10.1038/ncomms13603, 2016.
Meyer, H., Chapligin, B., Hoff, U., Nazarova, L., and Diekmann, B.: Oxygen isotope composition of diatoms as Late Holocene climate proxy at Two-Yurts Lake, Central Kamchatka, Russia, Global Planet Change, 134, 118-128, 10.1016/j.gloplacha.2014.04.008, 2015a.
Meyer, H., Opel, T., Laepple, T., Dereviagin, A. Y., Hoffmann, K., and Werner, M.: Long-term winter warming trend in the Siberian Arctic during the mid- to late Holocene, Nature Geoscience, 8, 122-125, 10.1038/ngeo2349, 2015b.
Meyer, H., Kostrova, S. S., Meister, P., Lenz, M. M., Kuhn, G., Nazarova, L., Syrykh, L. S., and Dvornikov, Y.: Lacustrine diatom oxygen isotopes as palaeo precipitation proxy - Holocene environmental and snowmelt variations recorded at Lake Bolshoye Shchuchye, Polar Urals, Russia, Quaternary Sci Rev, 290, 107620, https://doi.org/10.1016/j.quascirev.2022.107620, 2022.
Morley, D. W., Leng, M. J., Mackay, A. W., and Sloane, H. J.: Late glacial and Holocene environmental change in the Lake Baikal region documented by oxygen isotopes from diatom silica, Global Planet Change, 46, 221-233, 10.1016/j.gloplacha.2004.09.018, 2005.
Morley, D. W., Leng, M. J., Mackay, A. W., Sloane, H. J., Rioual, P., and Battarbee, R. W.: Cleaning of lake sediment samples for diatom oxygen isotope analysis, J Paleolimnol, 31, 391-401, DOI 10.1023/B:JOPL.0000021854.70714.6b, 2004.
Moschen, R., Lücke, A., and Schleser, G. H.: Sensitivity of biogenic silica oxygen isotopes to changes in surface water temperature and palaeoclimatology, Geophys Res Lett, 32, https://doi.org/10.1029/2004GL022167, 2005.
Narancic, B., Pienitz, R., Chapligin, B., Meyer, H., Francus, P., and Guilbault, J.-P.: Postglacial environmental succession of Nettilling Lake (Baffin Island, Canadian Arctic) inferred from biogeochemical and microfossil proxies, Quaternary Sci Rev, 147, 391-405, 10.1016/j.quascirev.2015.12.022, 2016.
Neukom, R., Steiger, N., Gómez-Navarro, J. J., Wang, J., and Werner, J. P.: No evidence for globally coherent warm and cold periods over the preindustrial Common Era, Nature, 571, 550-554, 10.1038/s41586-019-1401-2, 2019.

Opel, T., Wetterich, S., Meyer, H., Dereviagin, A. Y., Fuchs, M. C., and Schirrmeister, L.: Ground-ice stable isotopes and cryostratigraphy reflect late Quaternary palaeoclimate in the Northeast Siberian Arctic (Oyogos Yar coast, Dmitry Laptev Strait), Clim. Past, 13, 587-611, 10.5194/cp-13-587-2017, 2017.

Pfalz, G., Diekmann, B., Freytag, J.-C., and Biskaborn, B. K.: Harmonizing heterogeneous multi-proxy data from lake systems, Computers & Geosciences, 153, 104791, https://doi.org/10.1016/j.cageo.2021.104791, 2021.

Polissar, P., Abbott, M., Shemesh, A., Wolfe, A., and Bradley, R.: Holocene hydrologic balance of tropical South America from oxygen isotopes of lake sediment opal, Venezuelan Andes, Earth Planet Sc Lett, 242, 375-389, 10.1016/j.epsl.2005.12.024, 2006.

Quesada, B., Sylvestre, F., Vimeux, F., Black, J., Paillès, C., Sonzogni, C., Alexandre, A., Blard, P.-H., Tonetto, A., Mazur, J.-C., and Bruneton, H.: Impact of Bolivian paleolake evaporation on the δ18O of the Andean glaciers during the last deglaciation (18.5–11.7 ka): diatom-inferred δ18O values and hydro-isotopic modeling, Quaternary Sci Rev, 120, 93-106, 10.1016/j.quascirev.2015.04.022, 2015.

Renssen, H., Seppä, H., Heiri, O., Roche, D. M., Goosse, H., and Fichefet, T.: The spatial and temporal complexity of the Holocene thermal maximum, Nature Geoscience, 2, 411-414, 10.1038/ngeo513, 2009.

Rietti-Shati, M., Shemesh, A., and Karlen, W.: A 3000-Year Climatic Record from Biogenic Silica Oxygen Isotopes in an Equatorial High-Altitude Lake, Science, 281, 980-982, 10.1126/science.281.5379.980, 1998.

Rosqvist, G., Rietti-Shati, M., and Shemesh, A.: Late Glacial to middle Holocene climatic record of lacustrine biogenic silica oxygen isotopes from a Southern Ocean Island, Geology, 27, 10.1130/0091-7613(1999)027<0967:LGTMHC>2.3.CO;2, 1999.

Rosqvist, G., Jonsson, C., Yam, R., Karlen, W., and Shemesh, A.: Diatom oxygen isotopes in pro-glacial lake sediments from northern Sweden: a 5000 year record of atmospheric circulation, Quaternary Sci Rev, 23, 851-859, 10.1016/j.quascirev.2003.06.009, 2004.

Rosqvist, G. C., Leng, M. J., Goslar, T., Sloane, H. J., Bigler, C., Cunningham, L., Dadal, A., Bergman, J., Berntsson, A., Jonsson, C., and Wastegård, S.: Shifts in precipitation during the last millennium in northern Scandinavia from lacustrine isotope records, Quaternary Sci Rev, 66, 22-34, 10.1016/j.quascirev.2012.10.030, 2013.

Rozanski, K., Klisch, M. A., Wachniew, P., Gorczyca, Z., Goslar, T., Edwards, T. W. D., and Shemesh, A.: Oxygen-isotope geothermometers in lacustrine sediments: New insights through combined δ18O analyses of aquatic cellulose, authigenic calcite and biogenic silica in Lake Gościąż, central Poland, Geochim Cosmochim Ac, 74, 2957-2969, 10.1016/j.gca.2010.02.026, 2010.

Ryves, D. B., Leng, M. J., Barker, P. A., Snelling, A. M., Sloane, H. J., Arrowsmith, C., Tyler, J. J., Scott, D. R., Radbourne, A. D., and Anderson, N. J.: Understanding the transfer of contemporary temperature signals into lake sediments via paired oxygen isotope ratios in carbonates and diatom silica: Problems and potential, Chem Geol, 552, ARTN 119705 10.1016/j.chemgeo.2020.119705, 2020.

Schiff, C., Kaufman, D., Wolfe, A., Dodd, J., and Sharp, Z.: Late Holocene storm-trajectory changes inferred from the oxygen isotope composition of lake diatoms, south Alaska, J Paleolimnol, 41, 189-208, 10.1007/s10933-008-9261-z, 2009.

Schmidt, M., Fuchs, M., Henderson, A. C. G., Kossler, A., Leng, M. J., Mackay, A. W., Shemang, E., and Riedel, F.: Paleolimnological features of a mega-lake phase in the Makgadikgadi Basin (Kalahari, Botswana) during Marine Isotope Stage 5 inferred from diatoms, J Paleolimnol, 58, 373-390, 10.1007/s10933-017-9984-9, 2017.

Shemesh, A. and Peteet, D.: Oxygen isotopes in fresh water biogenic opal - Northeastern US Alleröd-Younger Dryas temperature shift, Geophys Res Lett, 25, 1935-1938, 10.1029/98gl01443, 1998.

Shemesh, A., Rosqvist, G., Rietti-Shati, M., Rubensdotter, L., Bigler, C., Yam, R., and Karlén, W.: Holocene climatic change in Swedish Lapland inferred from an oxygen-isotope record of lacustrine biogenic silica, The Holocene, 11, 447-454, 10.1191/095968301678302887, 2001a.

Shemesh, A., Rietti-Shati, M., Rioual, P., Battarbee, R., de Beaulieu, j.-L., Reille, M., Andrieu-Ponel, V., and Svitavská - Svobodová, H.: An oxygen isotope record of lacustrine opal from a European Maar indicates climatic stability during the Last Interglacial, Geophys Res Lett, 28, 2305-2308, 10.1029/2000GL012720, 2001b.

Smith, A. C., Leng, M. J., Swann, G. E. A., Barker, P. A., Mackay, A. W., Ryves, D. B., Sloane, H. J., Chenery, S. R. N., and Hems, M.: An experiment to assess the effects of diatom dissolution on oxygen isotope ratios, Rapid Commun Mass Sp, 30, 293-300, 10.1002/rcm.7446, 2016.

Spielhagen, R. F. and Mackensen, A.: Upper ocean variability off NE Greenland (79°N) since the last glacial maximum reconstructed from stable isotopes in planktic foraminifer morphotypes, Quaternary Sci Rev, 265, 107070, https://doi.org/10.1016/j.quascirev.2021.107070, 2021.

Street-Perrott, F. A., Barker, P. A., Leng, M. J., Sloane, H. J., Wooller, M. J., Ficken, K. J., and Swain, D. L.: Towards an understanding of late Quaternary variations in the continental biogeochemical cycle of silicon: multi-isotope and sediment-flux data for Lake Rutundu, Mt Kenya, East Africa, since 38 ka BP, J Quaternary Sci, 23, 375-387, 10.1002/jqs.1187, 2008.

Subetto, D. A., Nazarova, L. B., Pestryakova, L. A., Syrykh, L. S., Andronikov, A. V., Biskaborn, B., Diekmann, B., Kuznetsov, D. D., Sapelko, T. V., and Grekov, I. M.: Paleolimnological studies in Russian northern Eurasia: A review, Contemporary Problems of Ecology, 10, 327-335, 10.1134/S1995425517040102, 2017.

Swann, G. E. A., Leng, M. J., Juschus, O., Melles, M., Brigham-Grette, J., and Sloane, H. J.: A combined oxygen and silicon diatom isotope record of Late Quaternary change in Lake El'gygytgyn, North East Siberia, Quaternary Sci Rev, 29, 774-786, 10.1016/j.quascirev.2009.11.024, 2010.

https://doi.org/10.5194/cp-2022-96
Preprint. Discussion started: 24 January 2023

Swann, G. E. A., Mackay, A. W., Vologina, E., Jones, M. D., Panizzo, V. N., Leng, M. J., Sloane, H. J., Snelling, A. M., and Sturm, M.: Lake Baikal isotope records of Holocene Central Asian precipitation, Quaternary Sci Rev, 189, 210-222, 10.1016/j.quascirev.2018.04.013, 2018.

Tyler, J. J., Sloane, H. J., Rickaby, R. E. M., Cox, E. J., and Leng, M. J.: Post-mortem oxygen isotope exchange within cultured diatom silica, Rapid Commun Mass Sp, 31, 1749-1760, 10.1002/rcm.7954, 2017.

Vinther, B. M., Buchardt, S. L., Clausen, H. B., Dahl-Jensen, D., Johnsen, S. J., Fisher, D. A., Koerner, R. M., Raynaud, D., Lipenkov, V., Andersen, K. K., Blunier, T., Rasmussen, S. O., Steffensen, J. P., and Svensson, A. M.: Holocene thinning of the Greenland ice sheet, Nature, 461, 385-388, 10.1038/nature08355, 2009.

Vyse, S. A., Herzschuh, U., Andreev, A. A., Pestryakova, L. A., Diekmann, B., Armitage, S. J., and Biskaborn, B. K.: Geochemical and sedimentological responses of arctic glacial Lake Ilirney, chukotka (far east Russia) to palaeoenvironmental change since ~51.8 ka BP, Quaternary Sci Rev, 247, 106607, https://doi.org/10.1016/j.quascirev.2020.106607, 2020.

WILSON, K. E., LENG, M. J., and MACKAY, A. W.: The use of multivariate statistics to resolve multiple contamination signals in the oxygen isotope analysis of biogenic silica, J Quaternary Sci, 29, 641-649, https://doi.org/10.1002/jqs.2729, 2014a.

Wilson, K. E., Maslin, M. A., Leng, M. J., Kingston, J. D., Deino, A. L., Edgar, R. K., and Mackay, A. W.: East African lake evidence for Pliocene millennial-scale climate variability, Geology, 42, 955-958, 10.1130/g35915.1, 2014b.

Wolfe, B. B., Falcone, M. D., Clogg-Wright, K. P., Mongeon, C. L., Yi, Y., Brock, B. E., Amour, N. A. S., Mark, W. A., and Edwards, T. W. D.: Progress in isotope paleohydrology using lake sediment cellulose, J Paleolimnol, 37, 221-231, 10.1007/s10933-006-9015-8, 2007.